IAAF World Indoor Championships
BIRMINGHAM 2018
1–4 MARCH

BIOMECHANICAL REPORT

FOR THE

IAAF

WORLD INDOOR CHAMPIONSHIPS 2018

High Jump Men

Dr Gareth Nicholson, Dr Tim Bennett
and Dr Athanassios Bissas
Carnegie School of Sport

Stéphane Merlino
IAAF Project Leader

LBU LEEDS BECKETT UNIVERSITY

IAAF

Correspondence:

Dr Athanassios Bissas

Head of Sport & Exercise Biomechanics, Carnegie School of Sport

Leeds Beckett University

Fairfax Hall, Headingley Campus

Leeds, UK, LS6 3QT

Email: A.Bissas@leedsbeckett.ac.uk

Released:

February 2019

Please cite this report as:

Nicholson, G., Bennett, T. D., Bissas, A. and Merlino, S. (2019). *Biomechanical Report for the IAAF World Indoor Championships 2018: High Jump Men.* Birmingham, UK: International Association of Athletics Federations.

Event Director		Project Director
Dr Gareth Nicholson		Dr Athanassios Bissas
Project Coordinator		
Louise Sutton		
Senior Technical and Logistical Support		
Liam Gallagher	Aaron Thomas	Liam Thomas
Calibration	**Report Editors**	**Data Management**
Dr Brian Hanley	Josh Walker	Nils Jongerius
	Dr Catherine Tucker	Josh Walker
Data Analysts		
Dr Tim Bennett		Dr Gareth Nicholson
Project Team		
Dr Mark Cooke	Dr Alex Dinsdale	Helen Gravestock
	Dr Lysander Pollitt	
Masalela Gaesenngwe	Emily Gregg	Parag Parelkar
	Dr Giorgos Paradisis (*National and Kapodistrian University of Athens*)	
Scott Bingham	Iain Findlay	Dr Ian Richards
Jessica Thomas	Sarah Walker	Nathan Woodman
Coaching Commentary		
Denis Doyle		

Table of Contents

Figures

Tables

INTRODUCTION

The men's high jump final took place on the night of Thursday 1st March in the centre of the infield, back to back with the women's final, which took place simultaneously. Despite having cleared a world-leading 2.38 m in Tehran in early February, the reigning IAAF outdoor world champion Mutaz Essa Barshim from Qatar came into the event with some technical challenges. Meanwhile, Danil Lysenko competing as an authorised neutral athlete had registered lifetime bests on three occasions in the winter period leaping to 2.38 m in Hustopeče in late January. Although none of the Birmingham finalists surpassed their season's best, the high jump produced the first surprise of the championships. In a reversal from the 2017 contest in London, it was the world silver medallist Lysenko who leapt to victory above Barshim taking his first major international title. Both Lysenko and Barshim enjoyed first time clearances at 2.20 m, 2.25 m, 2.29 m and 2.33 m. Although Barshim was close to clearing 2.36 m in his second attempt, Lysenko produced a superb final leap to clear 2.36 m, just one centimetre short of his lifetime best. Despite coming into the competition ranked 13th in the 2018 world list, it was German's Mateusz Przybylko who claimed the bronze medal with a second-time clearance at 2.29 m. Przybylko fended off the close challenge of the 2012 Olympic medallist Erik Kynard who needed all three attempts to clear 2.29 m. The European indoor champion Sylwester Bednarek claimed fifth place with a first-time clearance of 2.25 m leaving Wang Yu of China, former world champion Donald Thomas (Bahamas) and the European junior champion Maksim Nedasekau (Belarus) in a tie for sixth place having all recorded first time clearances at 2.20 m.

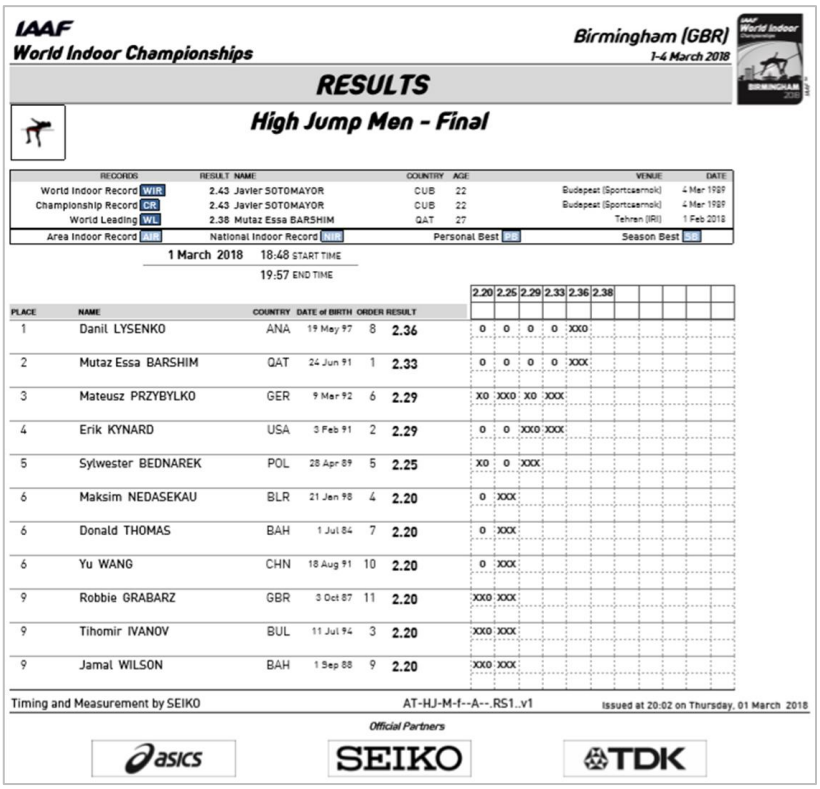

IAAF World Indoor Championships — Birmingham (GBR) 1-4 March 2018

RESULTS

High Jump Men - Final

RECORDS	RESULT	NAME	COUNTRY	AGE	VENUE	DATE
World Indoor Record WIR	2.43	Javier SOTOMAYOR	CUB	22	Budapest (Sportcsarnok)	4 Mar 1989
Championship Record CR	2.43	Javier SOTOMAYOR	CUB	22	Budapest (Sportcsarnok)	4 Mar 1989
World Leading WL	2.38	Mutaz Essa BARSHIM	QAT	27	Tehran (IRI)	1 Feb 2018

Area Indoor Record AIR — National Indoor Record NIR — Personal Best PB — Season Best SB

1 March 2018 18:48 START TIME

19:57 END TIME

PLACE	NAME	COUNTRY	DATE of BIRTH	ORDER	RESULT	2.20	2.25	2.29	2.33	2.36	2.38
1	Danil LYSENKO	ANA	19 May 97	8	2.36	o	o	o	o	xxo	
2	Mutaz Essa BARSHIM	QAT	24 Jun 91	1	2.33	o	o	o	o	xxx	
3	Mateusz PRZYBYLKO	GER	9 Mar 92	6	2.29	xo	xxo	xo	xxx		
4	Erik KYNARD	USA	3 Feb 91	2	2.29	o	o	xxo	xxx		
5	Sylwester BEDNAREK	POL	28 Apr 89	5	2.25	xo	o	xxx			
6	Maksim NEDASEKAU	BLR	21 Jan 98	4	2.20	o	xxx				
6	Donald THOMAS	BAH	1 Jul 84	7	2.20	o	xxx				
6	Yu WANG	CHN	18 Aug 91	10	2.20	o	xxx				
9	Robbie GRABARZ	GBR	3 Oct 87	11	2.20	xxo	xxx				
9	Tihomir IVANOV	BUL	11 Jul 94	3	2.20	xxo	xxx				
9	Jamal WILSON	BAH	1 Sep 88	9	2.20	xxo	xxx				

Timing and Measurement by SEIKO — AT-HJ-M-f--A--.RS1..v1 — Issued at 20:02 on Thursday, 01 March 2018

Official Partners: asics, SEIKO, TDK

METHODS

The landing mat for the men's high jump was positioned centrally in the arena back to back with the women's mat for which the competition took place concurrently. Three vantage locations for camera placement were identified and secured with each location having the capacity to accommodate at least one camera mounted on a tripod.

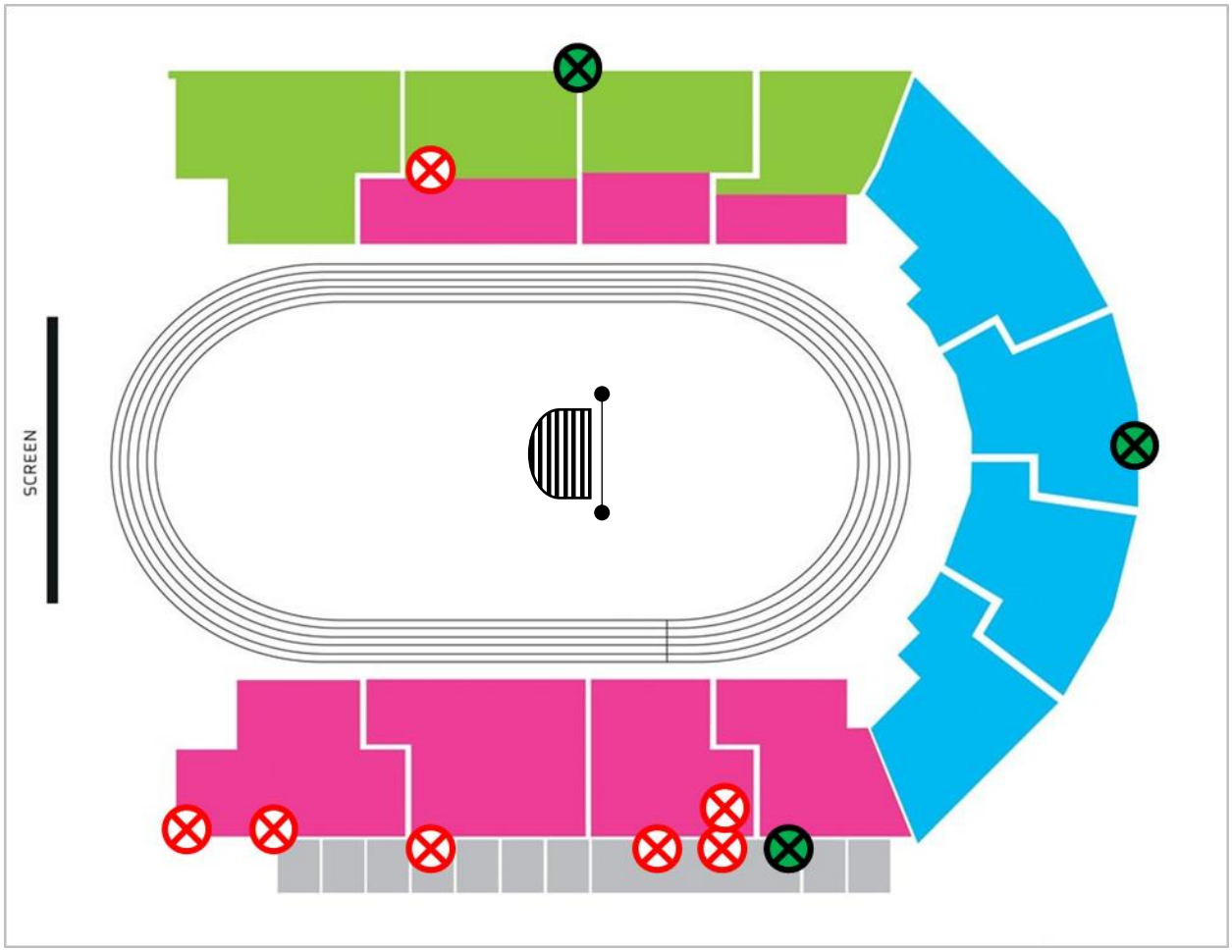

Figure 1. Camera layout for the men's high jump indicated by green-filled circles.

One standardised calibration procedure was conducted before and after the commencement of the events on the evening of the high jump. Specifically, a rigid cuboid calibration frame was filmed on the high jump run-up / take-off area and repositioned multiple times over discrete predefined areas. This ensured an accurate defined volume for athletes who approached the uprights from both left and right directions. This approach produced a large number of non-coplanar control points per individual calibrated volume and facilitated the construction of a three-dimensional global coordinate system.

A total of four high-speed cameras were employed to record the action during the men's high jump. Sony PXW-FS5 cameras operating at 200 Hz (shutter speed: 1/1250; ISO: 2000-4000; FHD: 1920x1080 px) were positioned strategically in pairs with their optical axes positioned to capture each athlete's attempt in all planes of movement. Separate camera pairings were utilised for athletes with left- and right-footed take-offs which enabled full-body motion capture to take place commencing three steps before take-off and ending when the athlete had landed.

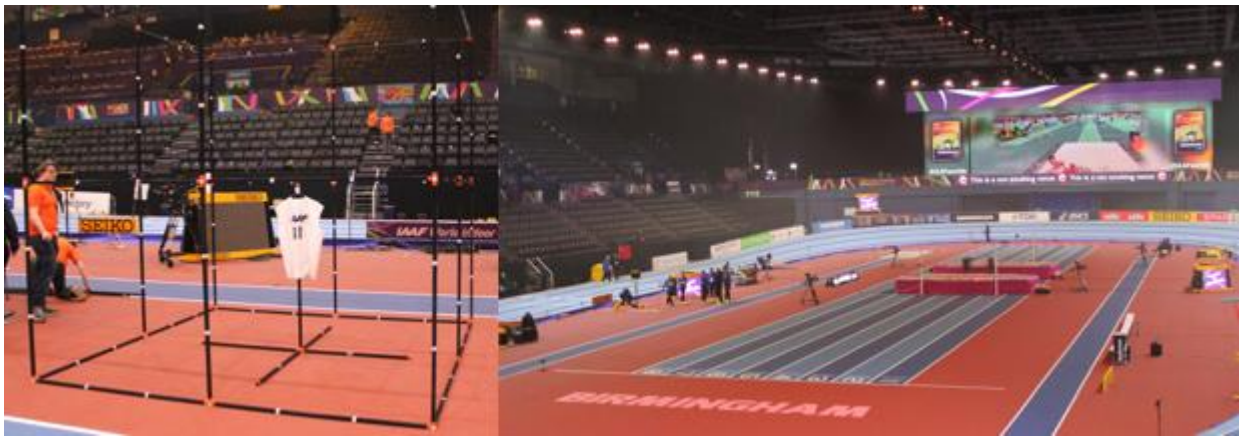

Figure 2. The calibration frame and position of the jump mat within the arena.

The video files were imported into SIMI Motion (SIMI Motion version 9.2.2, Simi Reality Motion Systems GmbH, Germany) and the highest successful attempt for each athlete was manually digitised by a single experienced operator to obtain kinematic data. An event synchronisation technique (synchronisation of four critical instants) was applied through SIMI Motion to synchronise the two-dimensional coordinates from each camera involved in the recording. Digitising started 15 frames before the beginning of the first touchdown and ended 15 frames after the required sequence to provide padding during filtering. Each file was first digitised frame by frame and upon completion adjustments were made as necessary using the points over frame method, where each point (e.g. right knee joint) was tracked through the entire sequence. The Direct Linear Transformation (DLT) algorithm was used to reconstruct the real-world 3D coordinates from individual camera's x and y image coordinates. Reliability of the digitising process was estimated by repeated digitising of one full trial with an intervening period of 48 hours. The results showed minimal systematic and random errors and therefore confirmed the high reliability of the digitising process. De Leva's (1996) body segment parameter models were used to obtain data for the whole body centre of mass and for key body segments. A recursive second-order, low-pass Butterworth digital filter (zero phase-lag) was employed to filter the raw coordinate data. The cut-off frequencies were calculated using residual analysis. Where available,

athletes' heights were obtained from 'Athletics 2017' (edited by Peter Matthews and published by the Association of Track and Field Statisticians) and online sources.

Figure 3. Action from the men's high jump final.

Each athlete's attempt was split into three consecutive parts:

1. *The approach:* from the instant at which the athlete begins approaching the bar until the instant of touchdown for the take-off.
2. *The take-off:* from the instant of touchdown (in the final contact) until the instant at which the take-off foot ends contact with the ground.
3. *The flight/ bar clearance:* from the instant of take-off until the instant of landing.

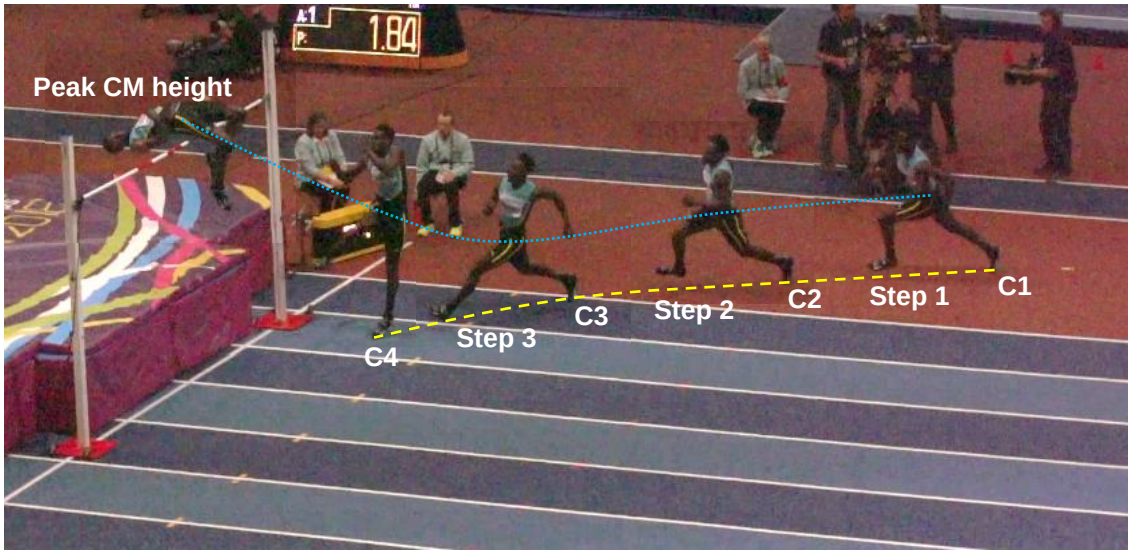

Figure 4. Key time-points at which the selected variables were obtained. C1-C4 denote foot contacts.

As the take-off conditions depend on the characteristics of the approach steps, the support and flight times, step lengths, centre of mass (CM) height, path of the centre of mass, angle of the run-up and horizontal / vertical velocities were computed for critical instants during athletes' run-up. With regards to take-off, the contact time, distance from the bar, body segment angles, take-off angle, horizontal / vertical velocities and location of the CM were computed (in some instances certain values could not be computed). To complete the analysis, the peak height of the CM and location of the peak CM height with respect to the bar was obtained. In addition to an in-depth understanding of the characteristics of each athlete's best jump, the aforementioned parameters enabled the attempts to split into the following three partial heights:

1. *H1:* the height of the CM at the instant of touchdown (TD) during the final contact.
2. *H2:* the height of the CM at the instant of toe-off (TO) during the take-off phase.
3. *H3:* the peak vertical height of the CM during flight.

Table 1. Definitions of variables.

Variable	Definition
CM height	The vertical height of the CM at TD and TO during the final foot contact.
∆ TO height (%)	The change in CM height from TD to TO during the take-off phase (expressed as a percentage of CM height at TD).
Peak CM location	The anteroposterior distance of the CM from the bar at the instant of peak CM height.
Peak pelvis height	The maximum vertical height of the pelvis during flight.
PPH diff	The difference between peak pelvis height and the mark attained.
Path of run-up	The overhead representation of the path of the foot contacts during the last three approach steps.
CM attack angle at TO	The angle between the peak CM position over the bar and the CM position at final take-off (viewed overhead).
Step to bar angle at foot contacts 1-3	The angle between each respective foot contact relative to the bar.
CM-foot distance at TD	The horizontal distance (resultant) between the CM and plant foot CM at the instant of TD during the take-off phase.

Horizontal distance travelled during flight	The horizontal distance (resultant) between the CM at TO (during the take-off phase) and the CM at peak height (during the flight phase).
Take-off distance (TOD)	The foot-tip distance (anteroposterior) from the bar at take-off.
Step length (SL)	The displacement between toe-off of consecutive foot contacts.
Contact time (CT)	The time spent in contact with the ground during each foot contact.
Flight time (FT)	The time spent airborne during each step of the approach.
Ratio (FT/CT)	The flight time divided by the subsequent contact time.
Vertical velocity (V_v)	The vertical velocity of the CM at various time instants during the take-off phase.
Vertical velocity loss from peak	The percentage reduction in vertical velocity of the CM from the peak value to the value at TO.
Horizontal velocity (V_h)	The horizontal velocity (resultant of anteroposterior and mediolateral components) of the CM at various instants during take-off.
Resultant velocity (V_r)	The resultant velocity of the CM at various time instants.
Ratio of velocity change ($\Delta V_v / \Delta V_h$)	The change in vertical velocity relative to the change in horizontal velocity during the take-off phase.
Velocity transfer	The change in vertical velocity (from TD to TO) relative to the horizontal velocity at TD during the take-off phase.
Take-off angle	The angle of the CM relative to the horizontal at the instant of take-off (calculated from take-off velocities).
Hip angle at various time instants	The angle of the trunk relative to the shank at various time instances during the take-off and flight phase. (180° = full extension)
Knee angle at various time instants	The angle of the thigh relative to the shank at various time instances during the take-off phase. (180° = full extension)

Ankle angle at various time instants	The angle of the shank relative to the foot at various time instances during the take-off phase. (180° = full plantar flexion)
Joint velocities	The angular velocities of the hip, knee and ankle joints during the take-off phase (used to inform synchrony characteristics).
Knee flexion / extension duration	The time between maximum knee flexion and TD or TO during take-off.
Whole-body lean at TD	The angle of the line between the CM and ankle joint (take-off leg) relative to the vertical at TD and TO during the take-off phase.
Trunk lean at TD	The angle of the trunk relative to the vertical at TD during the take-off phase.
Shank angle at TD	The angle of the lower leg relative to the vertical and is considered to be 0^{o} when the shank is perpendicular to the running surface.
Hip-shoulder separation angle	The angle between a vector joining the right and left hips and a vector connecting the right and left shoulders.

Note: *CM = centre of mass.*

RESULTS

Table 2 below shows the highest clearance mark for each of the athletes and compares the mark to the season (2018) and personal best for each athlete.

Table 2. Best mark attained for each of the athletes expressed relative to their previous bests (before the Birmingham World Championships).

Athlete	Season's best (SB) (m)	Personal best (m)	Mark (m)	Difference from SB (%)
LYSENKO	2.37	2.37	2.36	−0.42
BARSHIM	2.38	2.41	2.33	−2.10
PRZYBYLKO	2.30	2.30	2.29	−0.43
KYNARD	2.31	2.34	2.29	−0.87
BEDNAREK	2.33	2.33	2.25	−2.10
NEDASEKAU	2.31	2.31	2.20	−4.76
THOMAS	2.31	2.33	2.20	−4.76
WANG	2.31	2.31	2.20	−4.76
GRABARZ	2.30	2.34	2.20	−4.35
IVANOV	2.28	2.28	2.20	−3.51
WILSON	2.31	2.31	2.20	−4.76

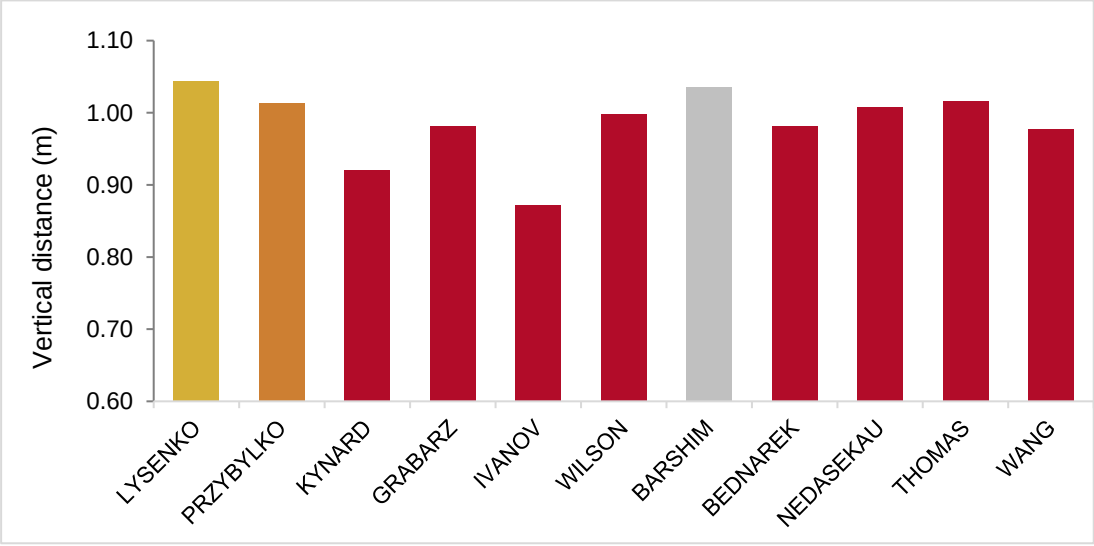

Figure 5. The difference in peak CM height and CM height at take-off for each athlete.

Figure 5 on the previous page shows the vertical distance that each athlete raised their CM from take-off to peak CM height during the flight phase. Table 3 below shows the individual and mean partial heights and also expresses these as a percentage of each athlete's standing height.

Table 3. Partial heights of the CM (in metres and relative to each athlete's stature) along with the peak CM location, peak pelvis height and PPH diff for each finalist. Each value rounded to 2 decimal places.

Athlete	H1 (m)	H2 (m)	H3 (m)	H3 diff (m)	H1 (%)	H2 (%)	H3 (%)	Peak CM location (m)	Peak pelvis height (m)	PPH diff (m)
LYSENKO	0.95	1.42	2.47	0.11	49.43	74.17	128.54	−0.22	2.55	0.19
BARSHIM	0.94	1.34	2.37	0.04	49.01	69.64	123.59	0.06	2.53	0.20
PRZYBYLKO	0.85	1.31	2.32	0.03	43.97	67.27	119.48	0.08	2.48	0.19
KYNARD	0.90	1.41	2.34	0.05	46.53	73.26	120.98	0.01	2.48	0.19
BEDNAREK	0.91	1.33	2.31	0.06	45.81	66.97	116.52	0.13	2.40	0.15
NEDASEKAU	0.90	1.29	2.30	0.10	-	-	-	−0.14	2.45	0.25
THOMAS	0.88	1.31	2.32	0.12	46.42	68.68	122.16	−0.06	2.45	0.25
WANG	0.90	1.25	2.22	0.02	46.98	64.95	115.83	0.01	2.37	0.17
GRABARZ	0.86	1.33	2.31	0.11	44.84	69.32	120.47	−0.12	2.45	0.25
IVANOV	0.99	1.39	2.26	0.06	49.85	70.25	114.29	0.10	2.43	0.23
WILSON	0.82	1.27	2.27	0.07	43.56	67.77	120.85	0.13	2.41	0.21

***Note**: Minus values for peak CM location indicate peak CM beyond the bar. H3 diff = H3 – mark attained.*

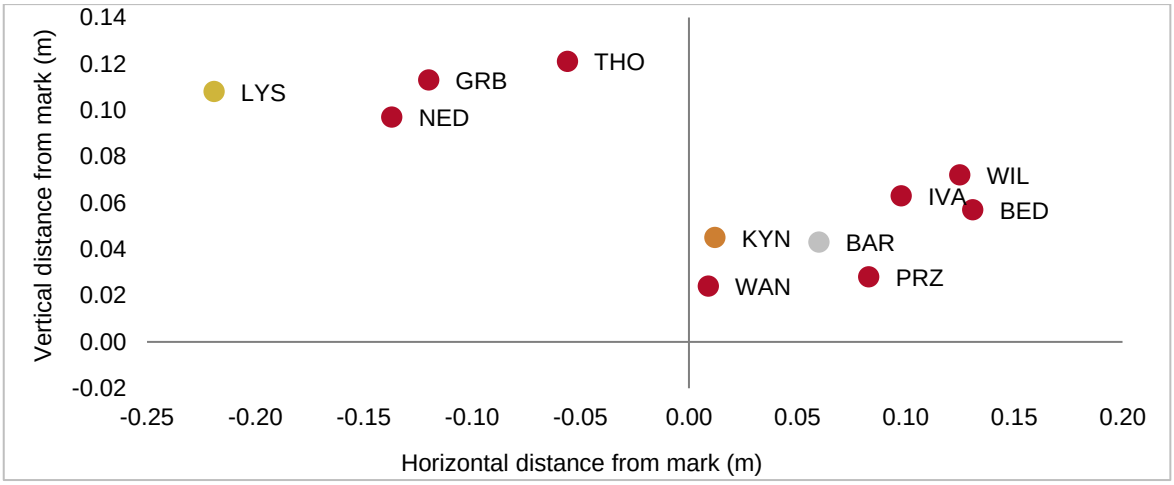

Figure 6. Scatterplot showing the distance of the CM (peak height) relative to the cleared mark in the vertical and horizontal directions. Minus values on the horizontal scale indicate area beyond the bar.

Figure 6 on the previous page shows the horizontal and vertical distance of the peak CM height from the bar for each finalist. The contrasting bar clearance techniques of the medallists should be considered when interpreting Figure 6 and Table 3 since this varied between the athletes. Table 4 below shows the hip angle at peak CM height for each of the athletes.

Table 4. Hip angle at peak CM height for each of the athletes.

Athlete	Hip angle at peak CM height (°)	
	Take-off limb	Free limb
LYSENKO	178	183
BARSHIM	217	239
PRZYBYLKO	249	204
KYNARD	207	230
BEDNAREK	206	196
NEDASEKAU	235	213
THOMAS	215	226
WANG	220	232
GRABARZ	200	226
IVANOV	230	225
WILSON	215	221

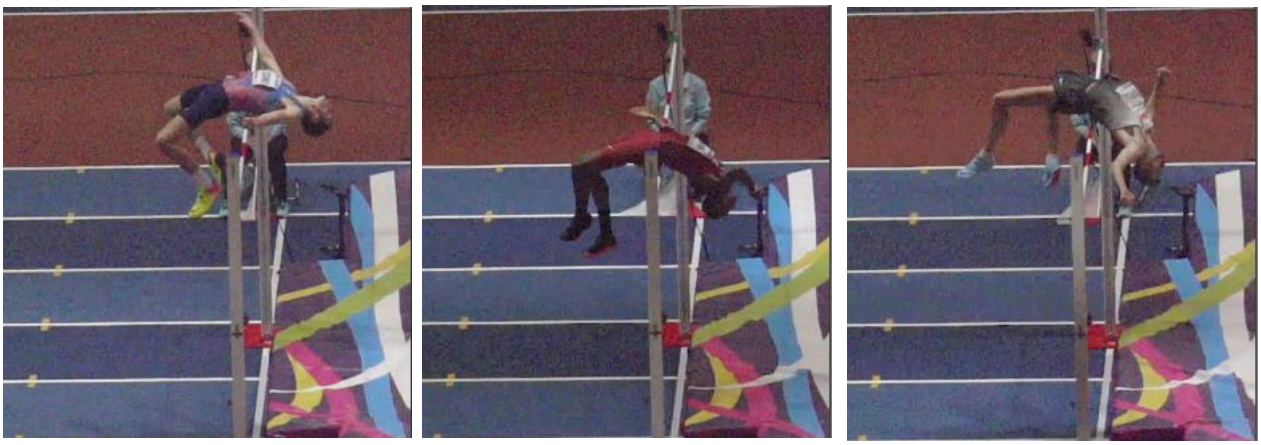

Figure 7. Contrasting bar clearance techniques of Lysenko (left), Barshim (centre), Przybylko (right). Please note: the images above do not correspond to peak CM height (and therefore the hip angles in Table 4).

Table 5 below shows the height of the CM at the instant of touchdown and take-off during the take-off phase along with the percentage lowering of the CM from touchdown to its lowest position. The table also shows the height of the CM at a) its lowest position and b) the point which the stance knee and free knee are parallel during the take-off phase. The CM reached its lowest position 0.03 seconds (on average) following touchdown whilst the knee reached parallel 0.07 seconds (on average) following touchdown. Figures 8 and 9 on the following page show the vertical position of the CM throughout the take-off phase for the medallists and other athletes.

Table 5. The height of the CM at final touchdown, at its lowest point, when the knees are parallel and at take-off (TO). The percentage lowering of the CM during take-off is also displayed (expressed relative to CM position at TD). Percentages are rounded to two decimal places.

Athlete	TD (m)	Lowest (m)	CM Lowering (%)	Knees Parallel (m)	TO (m)	Δ TO height (%)
LYSENKO	0.949	0.928	−2.21	0.984	1.424	50.05
BARSHIM	0.941	0.927	−1.49	1.006	1.337	42.08
PRZYBYLKO	0.853	0.841	−1.41	0.903	1.305	52.99
KYNARD	0.898	0.893	−0.56	0.950	1.414	57.46
BEDNAREK	0.907	0.905	−0.22	0.964	1.326	46.20
NEDASEKAU	0.896	0.876	−2.23	0.945	1.289	43.86
THOMAS	0.882	0.880	−0.23	0.935	1.305	47.96
WANG	0.902	0.870	−3.55	0.888	1.247	38.25
GRABARZ	0.861	0.859	−0.23	0.929	1.331	54.59
IVANOV	0.987	0.987	0.00	1.022	1.391	40.93
WILSON	0.819	0.799	−2.44	0.856	1.274	55.56

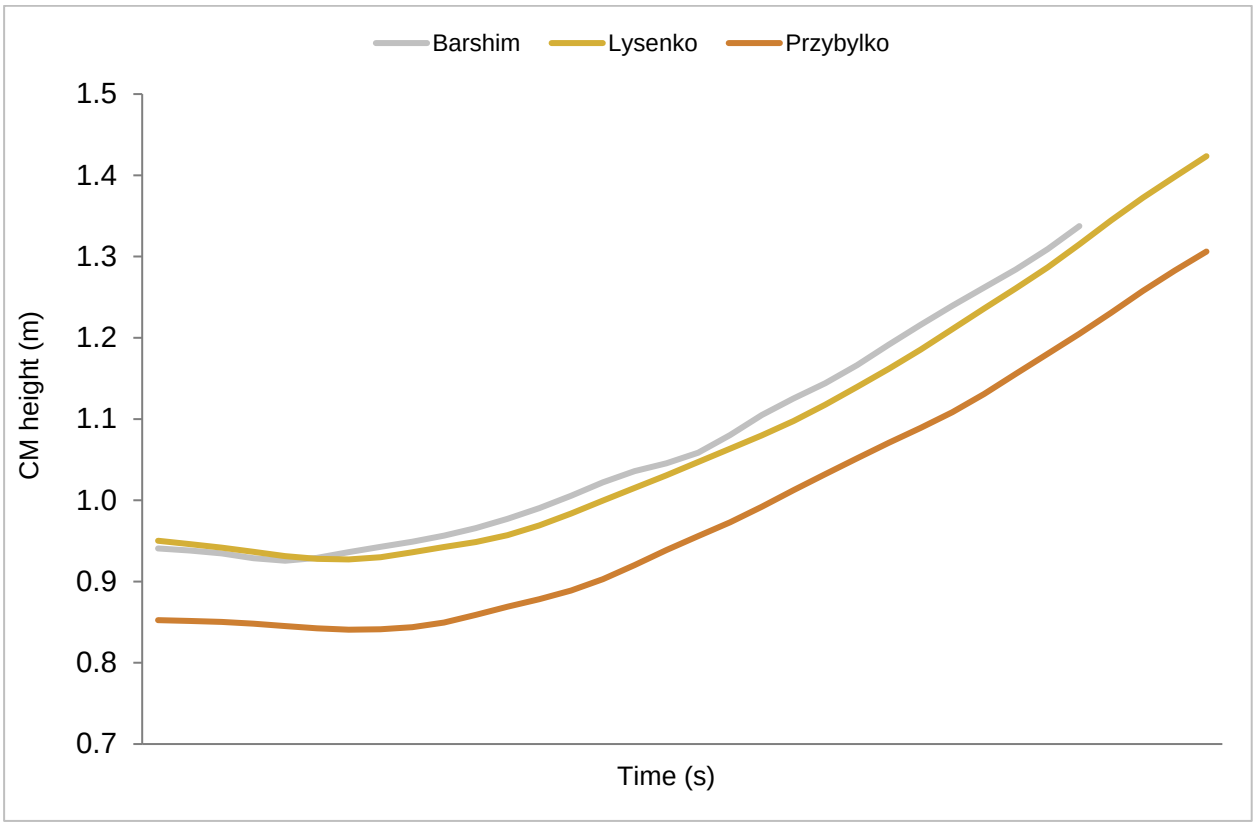

Figure 8. The vertical position of the CM during the take-off phase for the medallists.

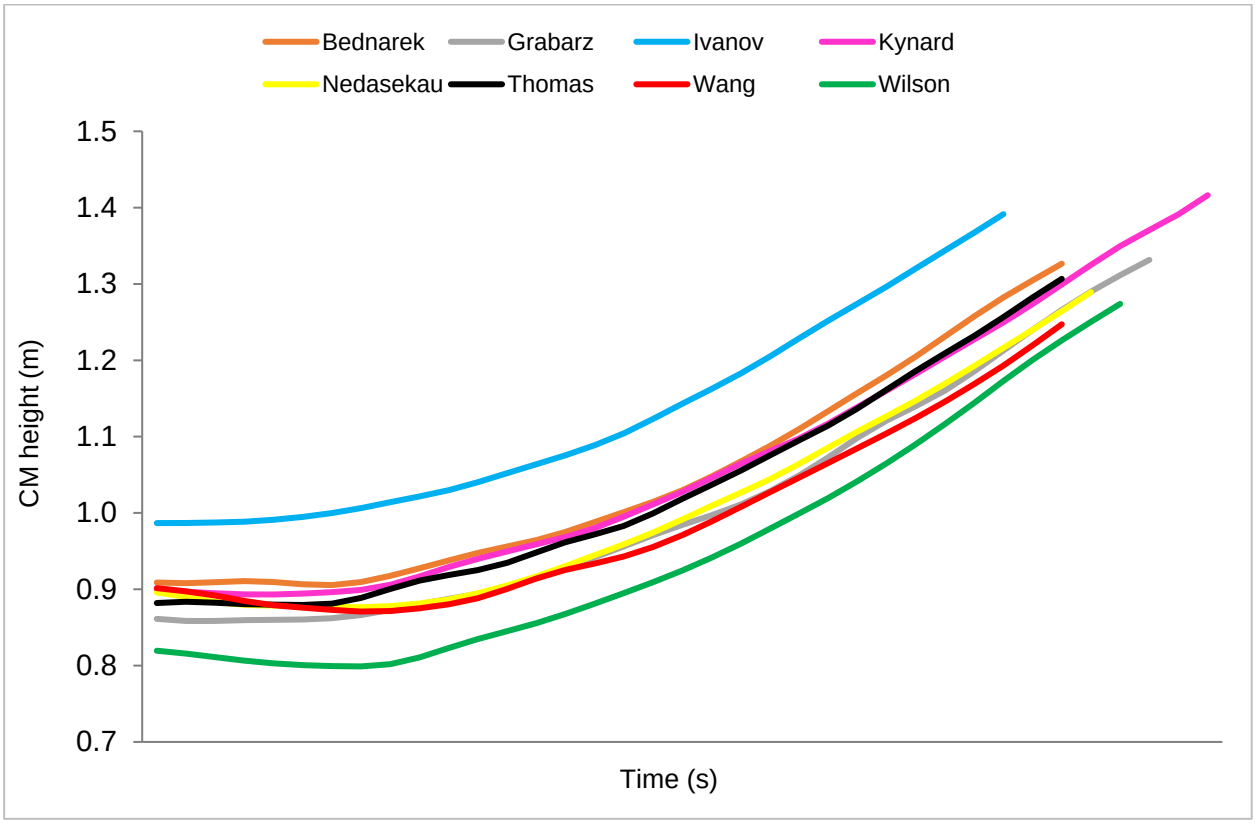

Figure 9. The vertical position of the CM during the take-off phase for the remaining athletes.

Table 6 below shows the horizontal velocity at final touchdown (TD) and take-off (TO) as well as the percentage change in horizontal velocity during the take-off phase.

Table 6. The horizontal velocity of the CM at final touchdown (TD) and take-off (TO) along with the change (%) in horizontal velocity during take-off (from TD to TO). Percentages are rounded to 2 decimal places.

Athlete	V_h at TD (m/s)	V_h at TO (m/s)	ΔV_h during take-off (%)
LYSENKO	7.37	4.34	−41.11
BARSHIM	7.66	4.40	−42.56
PRZYBYLKO	8.22	4.50	−45.26
KYNARD	7.83	4.57	−41.63
BEDNAREK	7.57	4.16	−45.05
NEDASEKAU	7.79	3.70	−52.50
THOMAS	7.63	4.10	−46.26
WANG	7.48	4.19	−43.98
GRABARZ	7.80	4.33	−44.49
IVANOV	7.36	4.47	−39.27
WILSON	7.33	3.43	−53.21

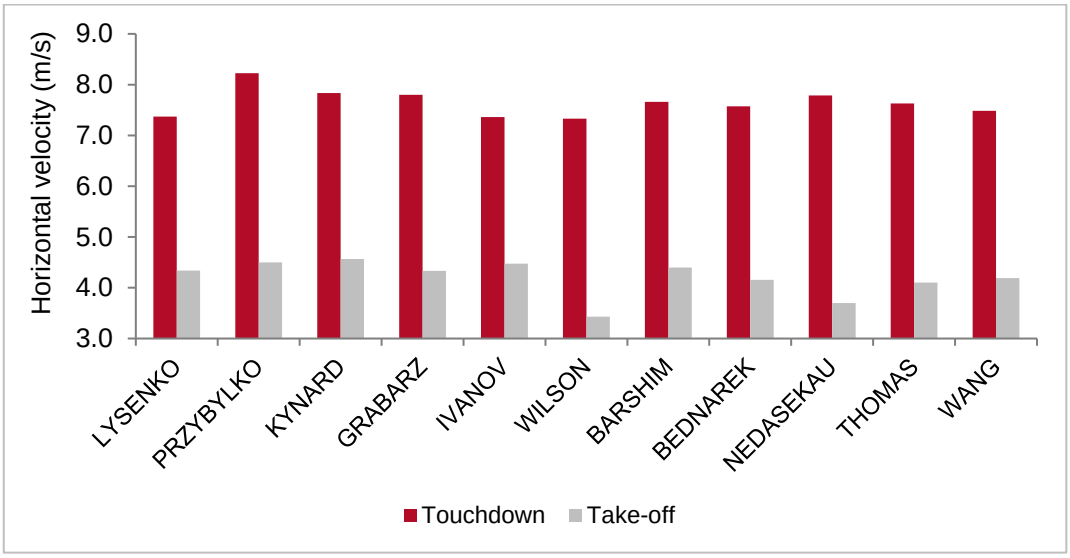

Figure 10. Horizontal velocity of the centre of mass at TD and TO for each of the athletes.

Figure 11 below shows the contrasting orientation and stability of the plant foot during the final foot contact for a number of the athletes.

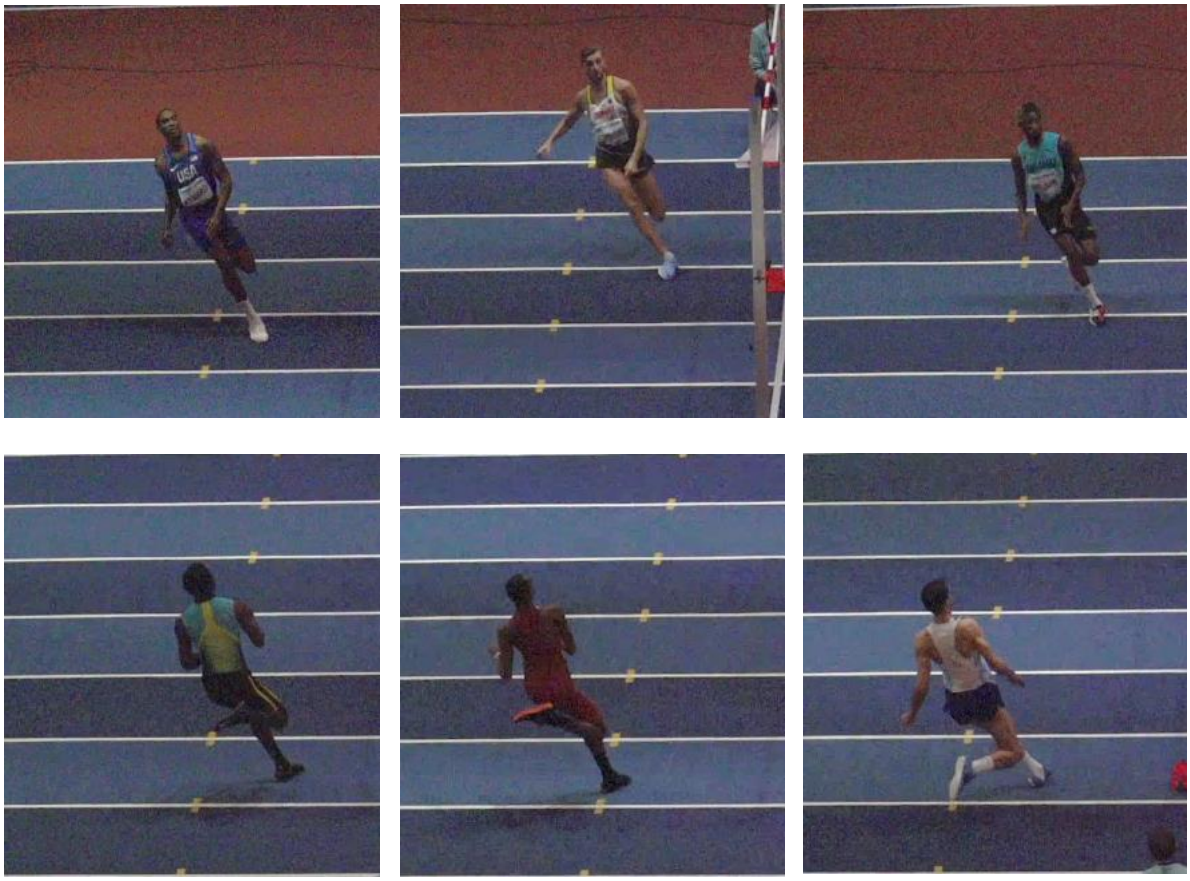

Figure 11. Contrasting levels of rear foot stability during take-off for a number of athletes.

Table 7 below shows the step-to-bar (SB) angles between each respective foot contact along with the percentage change from each angle to the next. Figure 12 shows how these angles were constructed and the angles are smaller for athletes who move more parallel to the bar. Table 7 also shows the CM attack angle with Figure 12 showing how this was constructed.

Table 7. Step-to-bar angle between toe-off to toe-off of each respective foot contact along with the percentage change in these angles from one to the next (1-3 indicates the % change from the first to the final angle).

Athlete	SB angle 1-2nd TO (°)	SB angle 2-3rd TO (°)	SB angle 3rd-4th TO (°)	Δ 1-2 (%)	Δ 2-3 (%)	Δ 1-3 (%)	CM attack angle TO (°)
LYSENKO	67.87	51.65	46.23	−23.90	−10.49	−31.88	39.79
BARSHIM	70.55	65.29	40.20	−7.46	−38.43	−43.02	55.29
PRZYBYLKO	57.93	48.41	21.89	−16.43	−54.78	−62.21	28.52
KYNARD	66.04	62.36	30.00	−5.57	−51.89	−54.57	42.91
BEDNAREK	70.98	55.29	22.89	−22.10	−58.60	−67.75	37.69
NEDASEKAU	-	47.67	28.38	-	−40.47	-	42.38
THOMAS	63.82	54.09	36.67	−15.25	−32.21	−42.54	41.94
WANG	57.60	47.74	30.95	−17.12	−35.17	−46.27	49.20
GRABARZ	67.01	51.59	25.46	−23.01	−50.65	−62.01	40.13
IVANOV	65.55	53.38	28.61	−18.57	−46.40	−56.35	40.98
WILSON	64.90	50.11	23.96	−22.79	−52.19	−63.08	34.23

***Note**: Certain values could not be computed for Nedasekau.*

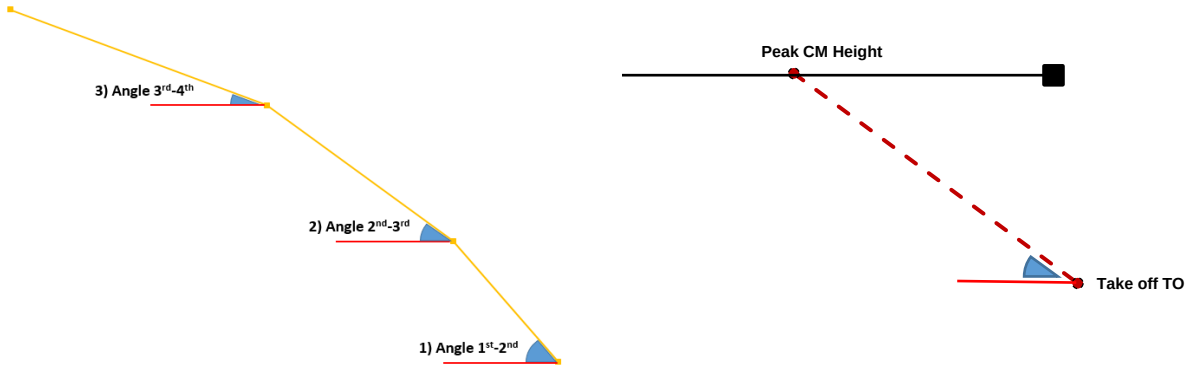

Figure 12. Schematic representation of the step-to-bar angle (left) and CM attack angle (right).

Figure 13 below shows an overhead view of the stance foot path during the approach for each athlete relative to the uprights (black solid line). Note: Athletes who utilised a right-foot take-off have been expressed as left-footers for the purpose of comparison.

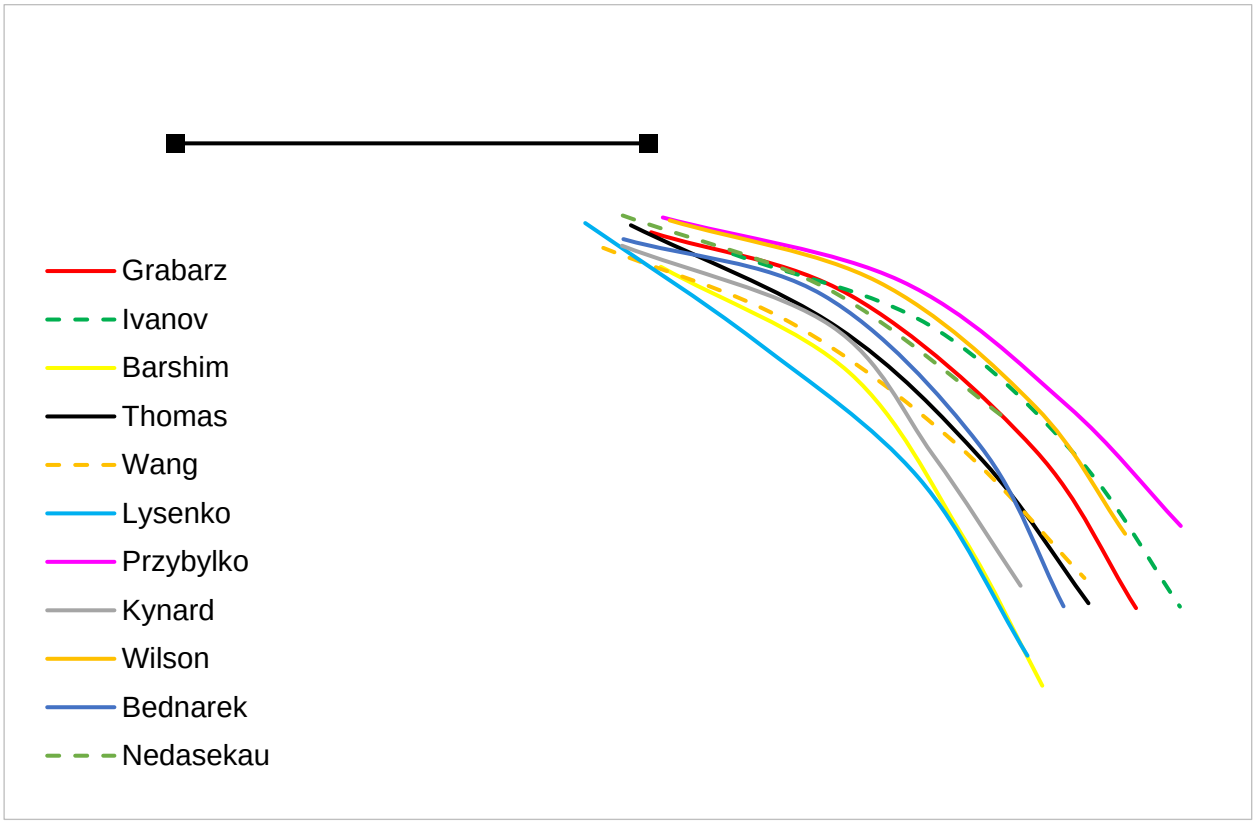

Figure 13. The overhead view of the paths of the stance foot during the approach and take-off.

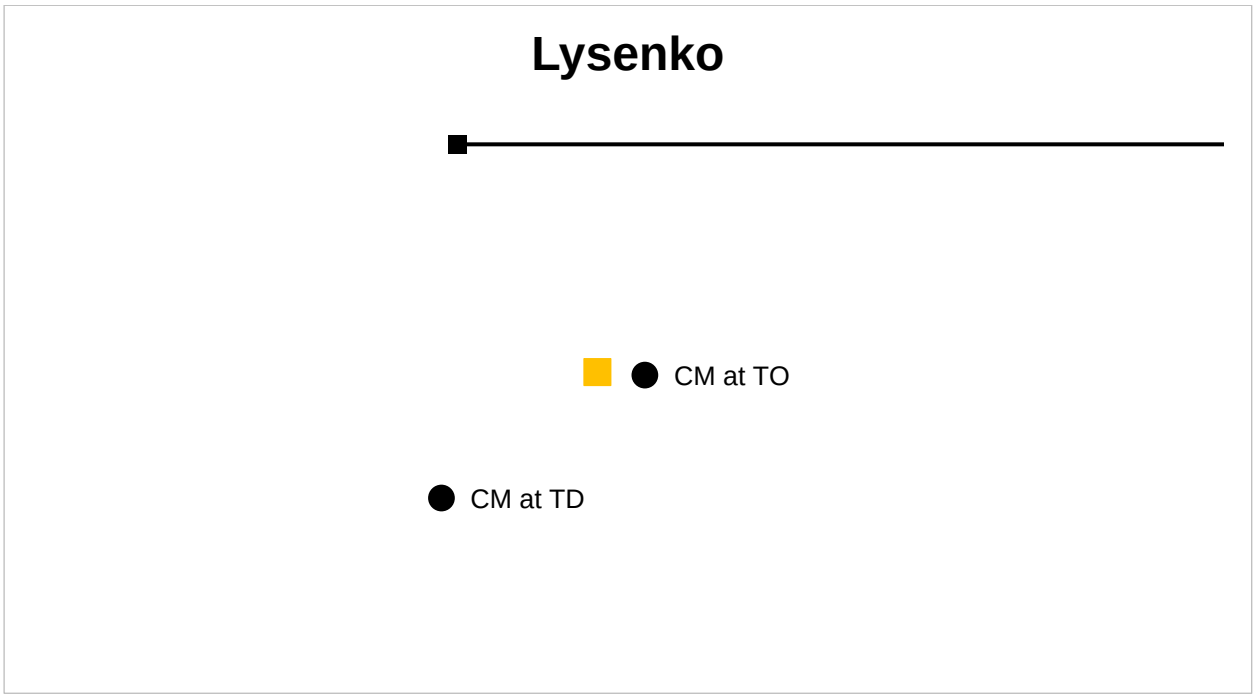

Figure 14. The overhead view of the CM and foot CM at TD and TO for Lysenko. Gold square indicates foot CM.

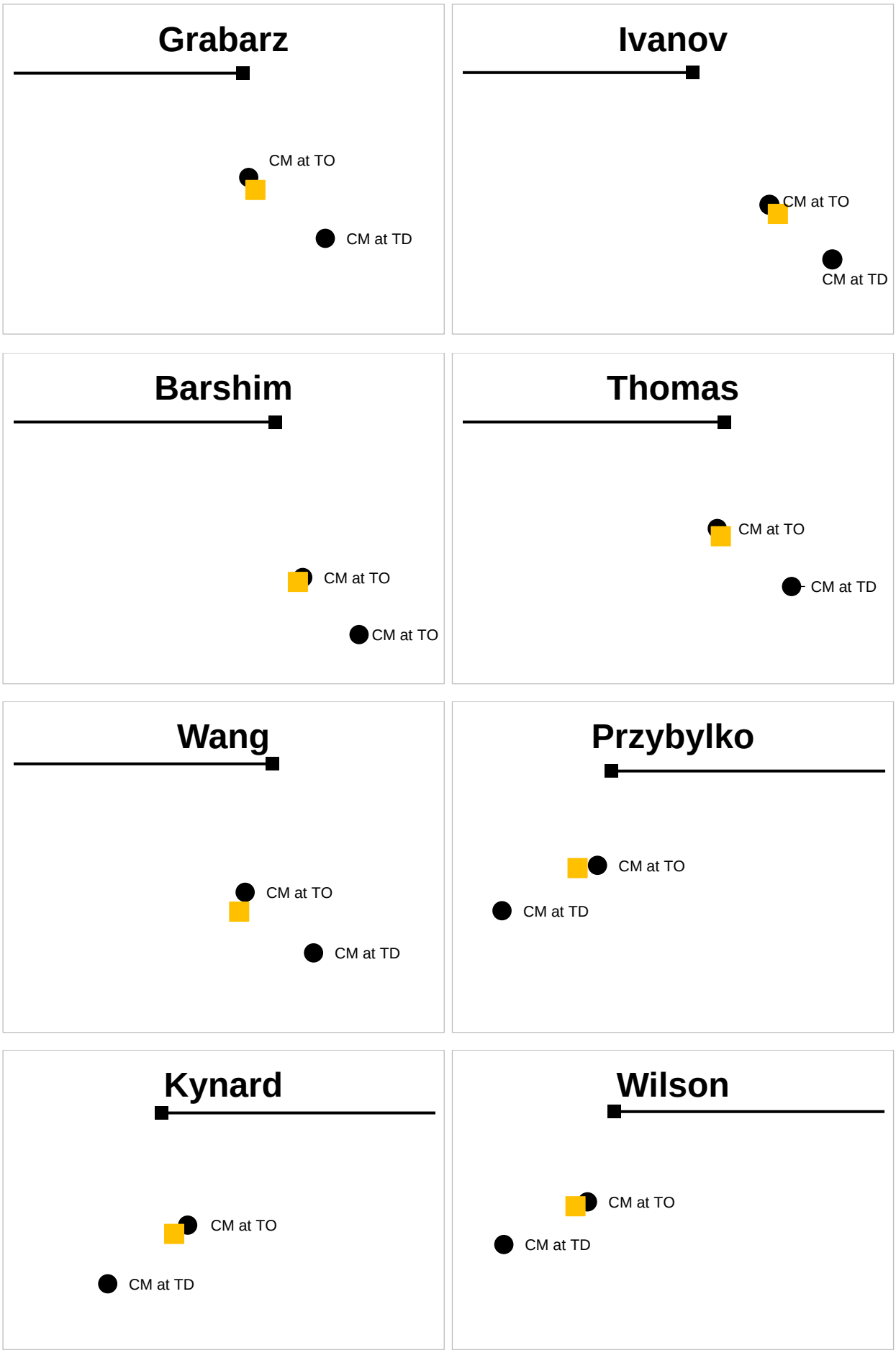
Grabarz
CM at TO
CM at TD
Ivanov
CM at TO
CM at TD
Barshim
CM at TO
CM at TO
Thomas
CM at TO
CM at TD
Wang
CM at TO
CM at TD
Przybylko
CM at TO
CM at TD
Kynard
CM at TO
CM at TD
Wilson
CM at TO
CM at TD

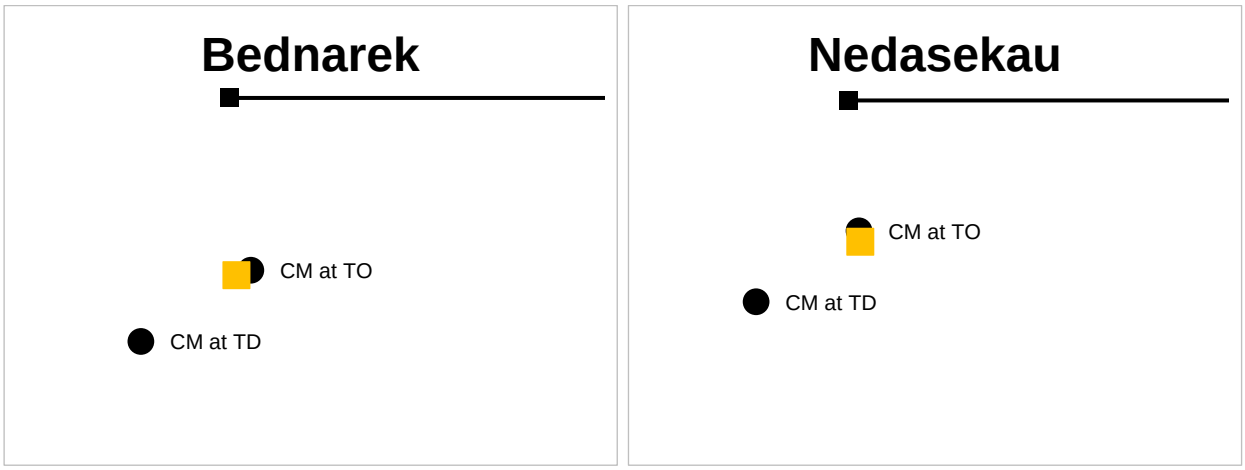

Figure 15. The overhead view of the CM and foot CM at TD and TO for the remaining athletes. Gold squares indicates foot CM.

This page shows the take-off distance, fight distance and whole-body CM to foot distance (at touchdown), these are explained in Figure 16 below and the values displayed in Table 8.

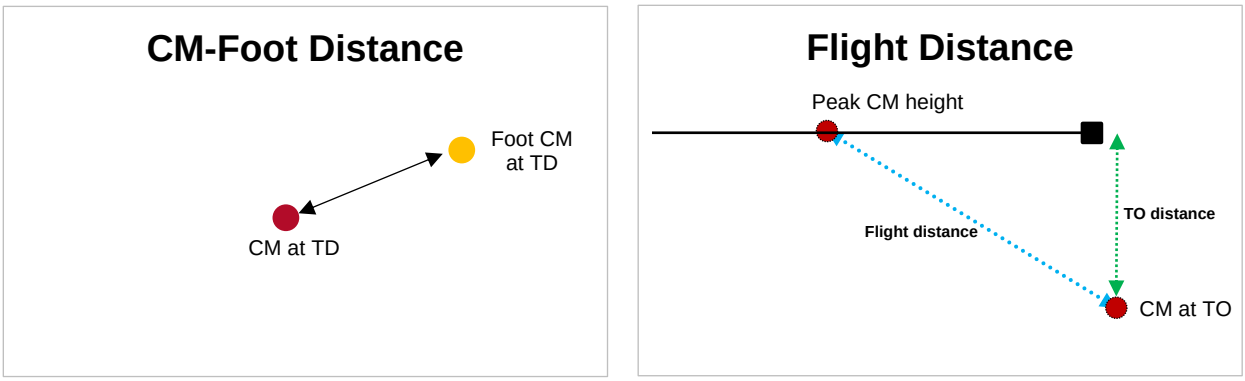

Figure 16. Left: Depiction of body CM to foot distance at TD. Right: Depiction of flight distance (blue line) and take-off distance (green line).

Table 8. Take-off distance (anteroposterior) and the horizontal flight distance (resultant) travelled from take-off to peak CM height. The horizontal distance between the CM and the stance foot at TD is also displayed (in metres and relative to stature).

Athlete	CM-foot distance at TD (m)	CM-foot distance at TD (%)	Flight distance (m)	Take-off distance (m)
LYSENKO	0.78	40.64	2.15	1.02
BARSHIM	0.75	38.99	1.92	1.54
PRZYBYLKO	0.78	40.12	1.92	0.93
KYNARD	0.80	41.37	1.88	1.28
BEDNAREK	0.76	38.31	1.90	1.21
NEDASEKAU	0.77	-	1.65	0.90
THOMAS	0.79	41.41	1.75	1.02
WANG	0.75	39.21	1.76	1.38
GRABARZ	0.81	42.05	1.88	1.12
IVANOV	0.70	35.46	1.97	1.40
WILSON	0.74	39.52	1.62	0.99

Table 9 and Figure 17 below show the length of the last three approach steps along with the duration of take-off for each of the finalists.

Table 9. The length of the last three approach steps along with the contact time of the take-off phase (CT) for the finalists. Step lengths are also expressed as a percentage of each athlete's stature.

Athlete	Step length (m)			Step length (%)			Δ 3-1 %	Take-off CT (s)
	1st step	2nd step	3rd step	1st step	2nd step	3rd step		
LYSENKO	2.44	2.20	2.08	127.30	114.57	108.48	−14.75	0.170
BARSHIM	2.01	2.29	2.08	104.62	119.48	108.21	3.48	0.150
PRZYBYLKO	1.82	2.10	2.16	93.56	108.48	111.32	18.68	0.170
KYNARD	1.81	1.86	2.03	93.60	96.16	105.41	12.15	0.185
BEDNAREK	2.15	2.33	1.82	108.77	117.78	92.05	−15.35	0.160
NEDASEKAU	-	2.16	1.97	-	-	-	-	0.165
THOMAS	2.01	2.10	2.17	106.04	110.35	113.97	7.96	0.160
WANG	2.03	2.08	1.83	105.74	108.10	95.41	−9.85	0.160
GRABARZ	2.19	2.50	1.86	113.84	130.35	96.80	−15.07	0.175
IVANOV	2.07	2.11	1.88	104.42	106.67	94.92	−9.18	0.155
WILSON	1.78	2.07	1.92	94.52	110.30	102.16	7.87	0.170

***Note**: Certain values could not be computed for Nedasekau.*

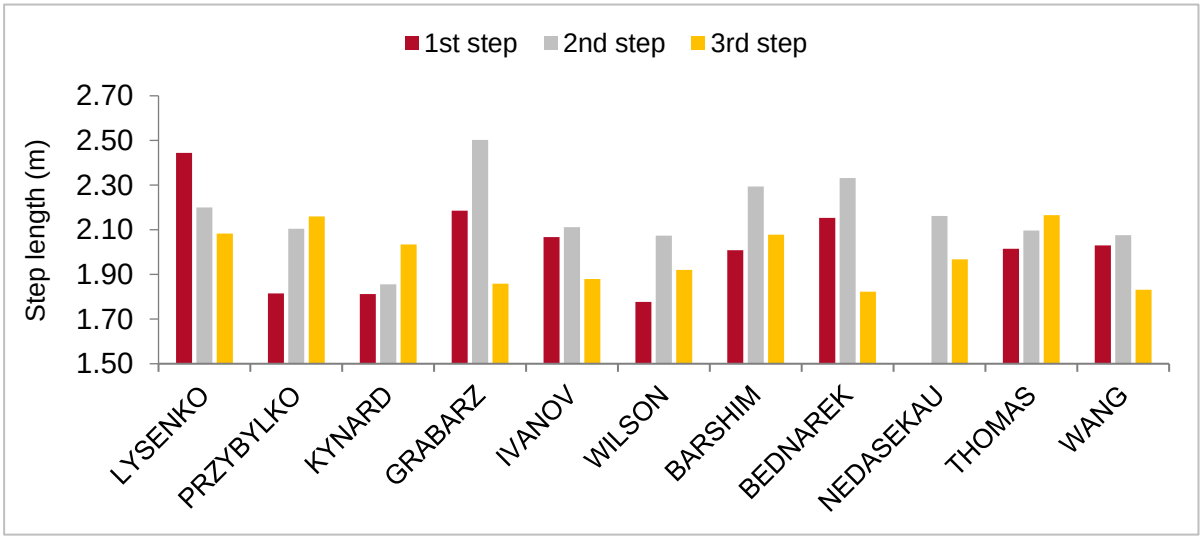

Figure 17. Length of the last three approach steps for each of the athletes.

Table 10 below shows the vertical and resultant velocities of the CM at key points during the take-off phase for each of the finalists along with various metrics showing the change in horizontal and vertical velocities with respect to each other.

Table 10. The vertical (V_v) and resultant (V_r) velocity values at TD and TO during the take-off phase along with the velocity transfer, take-off angle and the percentage loss in vertical velocity from peak to take-off.

Athlete	V_v at TD (m/s)	V_v at TO (m/s)	Loss from Peak-TO (%)	V_r at TO (m/s)	Velocity transfer (%)	Δ Ratio (V_v/V_h)	Take-off angle (°)
LYSENKO	−0.77	4.97	8.30	6.60	77.88	−1.90	49
BARSHIM	−0.77	4.81	1.84	6.52	72.85	−1.71	48
PRZYBYLKO	−0.36	4.72	5.22	6.52	61.80	−1.36	46
KYNARD	−0.29	4.63	3.74	6.51	62.84	−1.51	45
BEDNAREK	−0.15	4.68	5.26	6.26	63.80	−1.42	48
NEDASEKAU	−0.82	4.60	2.85	5.90	69.58	−1.33	51
THOMAS	−0.12	4.49	5.87	6.08	60.42	−1.31	48
WANG	−0.76	4.69	1.26	6.29	72.86	−1.66	48
GRABARZ	−0.65	4.34	12.15	6.13	63.97	−1.44	45
IVANOV	−0.06	4.58	2.66	6.40	63.04	−1.61	46
WILSON	−0.72	4.51	15.17	5.67	71.35	−1.34	53

Note: resultant velocities rounded to 2 decimal places.

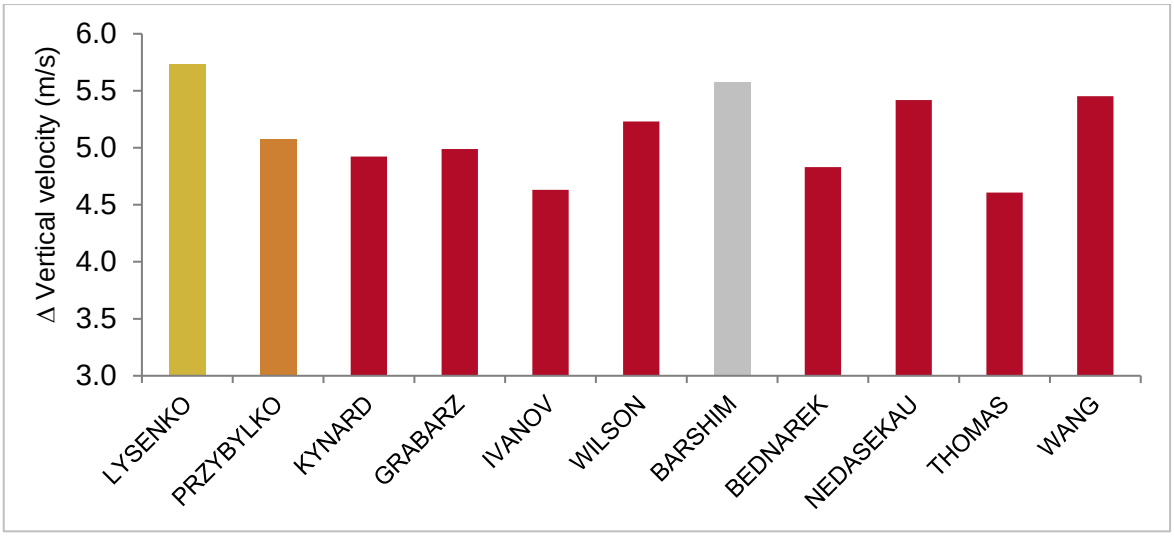

Figure 18. The gain in vertical velocity from TD to TO for each athlete.

Scatterplots showing the relationships between a) shank angle at TD and whole-body lean at TD and b) the vertical CM velocity at TO and the horizontal CM velocity at TD.

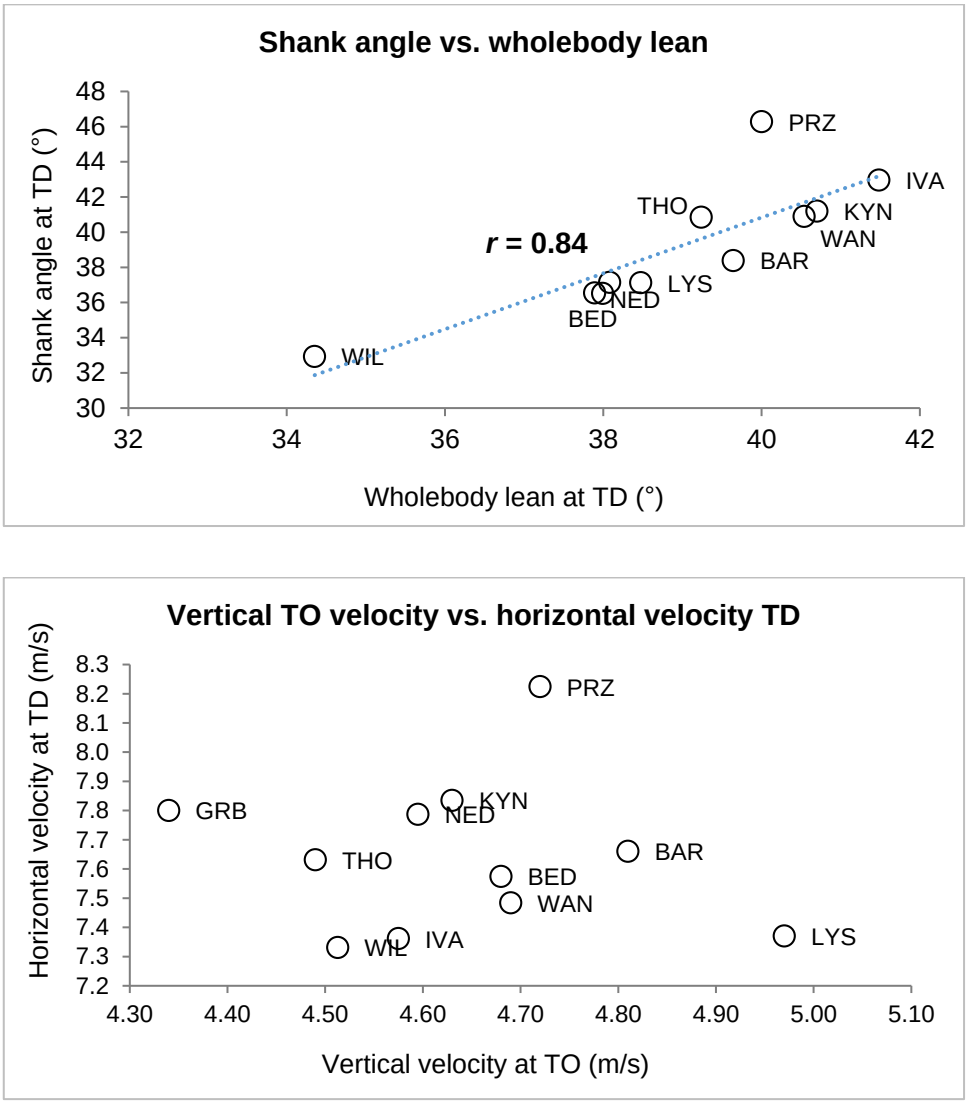

Figure 19. Relationships between key variables. *r* = correlation coefficient.

Table 11 below shows the angles of the knee and ankle (take-off leg) during the final foot contact for each of the athletes.

Table 11. The knee and ankle angles (for the take-off leg) at the instant of touchdown (TD) and take-off (TO) during the final foot contact (take-off phase) for all athletes. The lowest value is also displayed indicating peak flexion of these joints.

Athlete	Knee (°)			Ankle (°)		
	TD	Lowest	TO	TD	Lowest	TO
LYSENKO	170	151	176	127	110	141
BARSHIM	162	132	168	130	106	145
PRZYBYLKO	170	145	173	116	105	129
KYNARD	163	132	166	124	103	138
BEDNAREK	171	139	168	118	99	131
NEDASEKAU	171	144	170	120	109	151
THOMAS	162	140	171	116	113	139
WANG	164	131	170	113	103	143
GRABARZ	157	135	165	123	105	134
IVANOV	157	138	177	121	108	129
WILSON	159	136	163	116	100	124

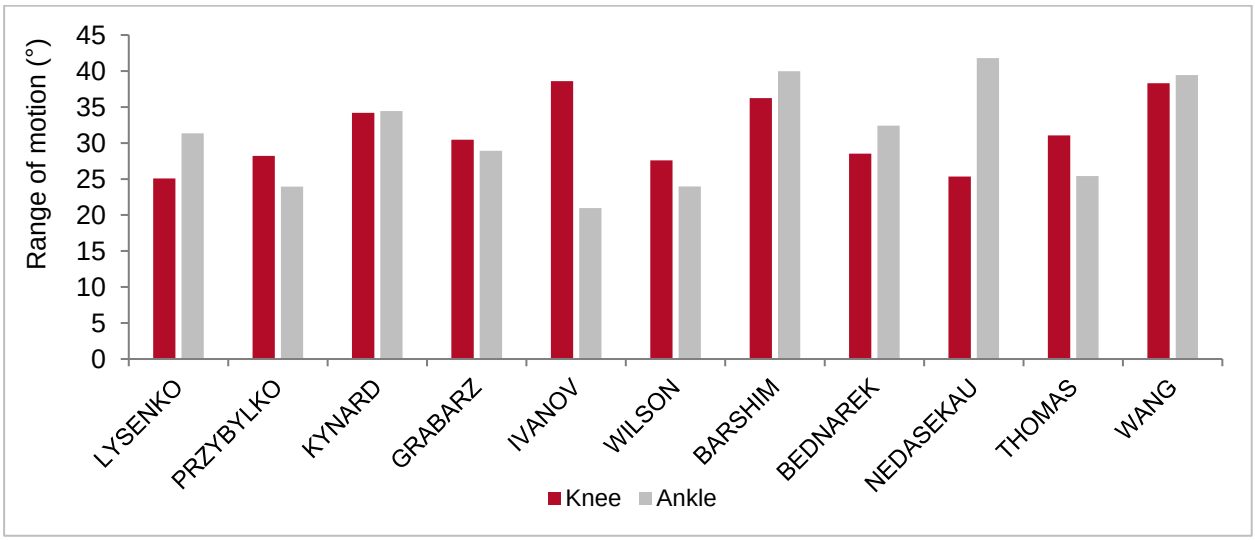

Figure 20. The range of motion of the knee and ankle (take-off leg) between maximum flexion and take-off for each athlete.

Figure 21 below provides an indication of the contact times and flight times for the final three approach steps. Note: contact 4 represents the duration of the take-off contact.

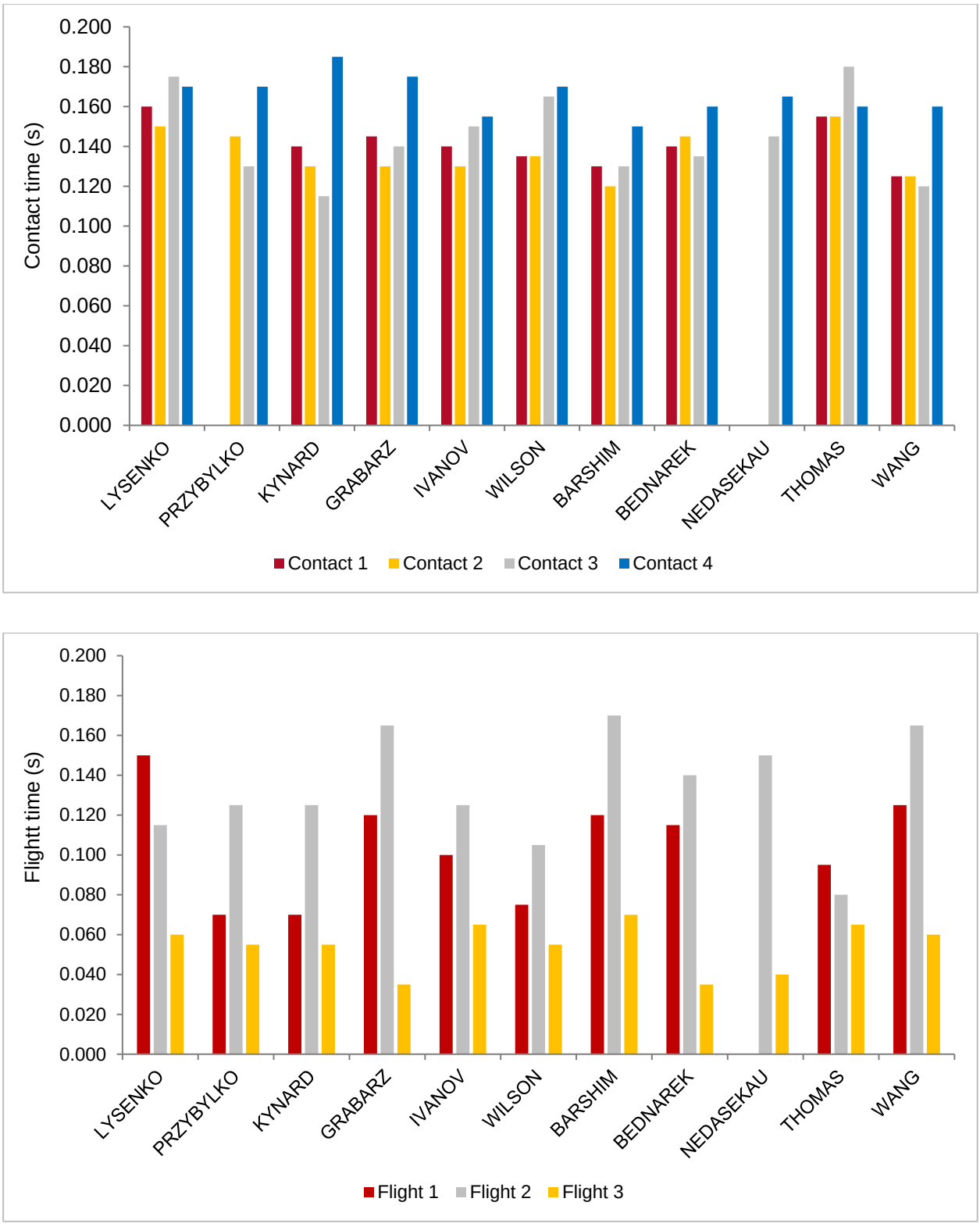

Figure 21. Top: Contact times for the final four ground contacts during the approach for each athlete. Bottom: Flight times for the final three steps before take-off (flight 3 precedes contact 4) for each athlete.

Figure 22 below shows the ratio of flight time to contact time (flight time divided by the subsequent contact time) during the final step for each of the athletes.

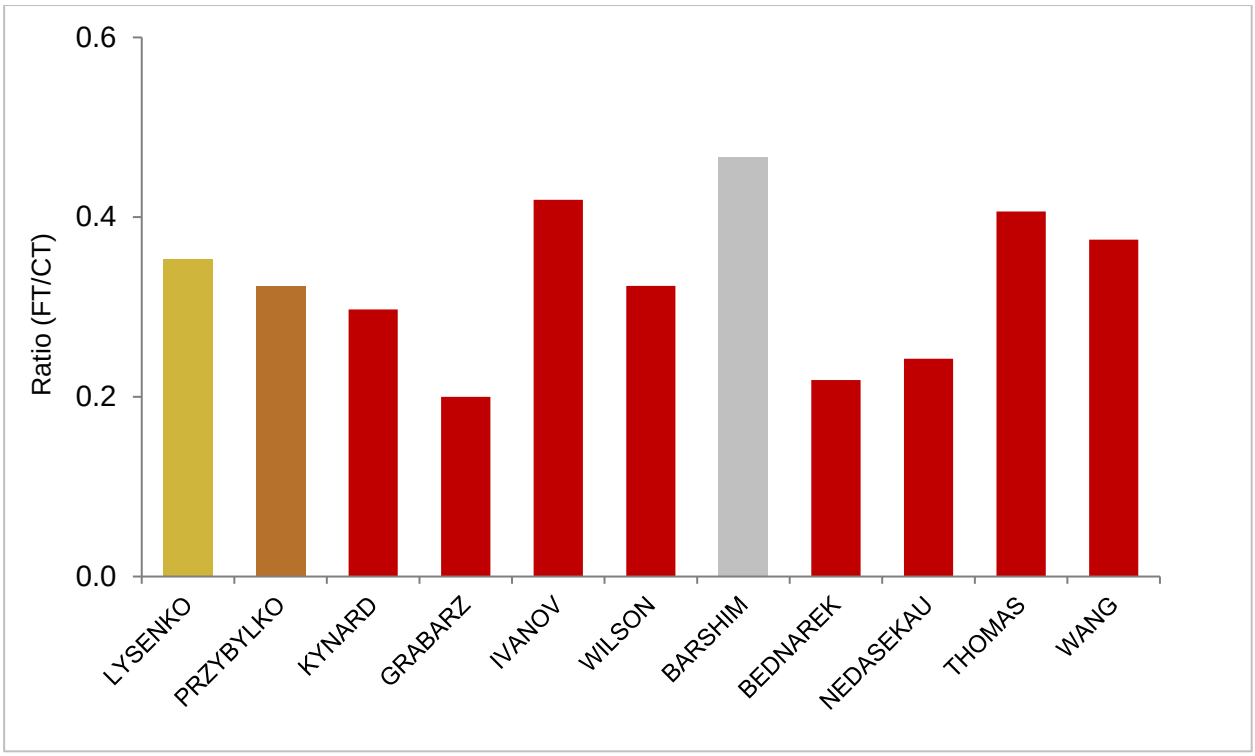

Figure 22. Ratio of flight time to ground contact time during the final step.

Table 12 and Figure 23 below show the time spent in knee flexion and extension during the final foot contact.

Table 12. The time spent in knee flexion and extension during the final foot contact.

Athlete	Flexion (s)	Extension (s)
LYSENKO	0.100	0.070
BARSHIM	0.085	0.065
PRZYBYLKO	0.110	0.060
KYNARD	0.130	0.055
BEDNAREK	0.085	0.075
NEDASEKAU	0.110	0.055
THOMAS	0.090	0.070
WANG	0.095	0.065
GRABARZ	0.095	0.080
IVANOV	0.070	0.085
WILSON	0.105	0.065

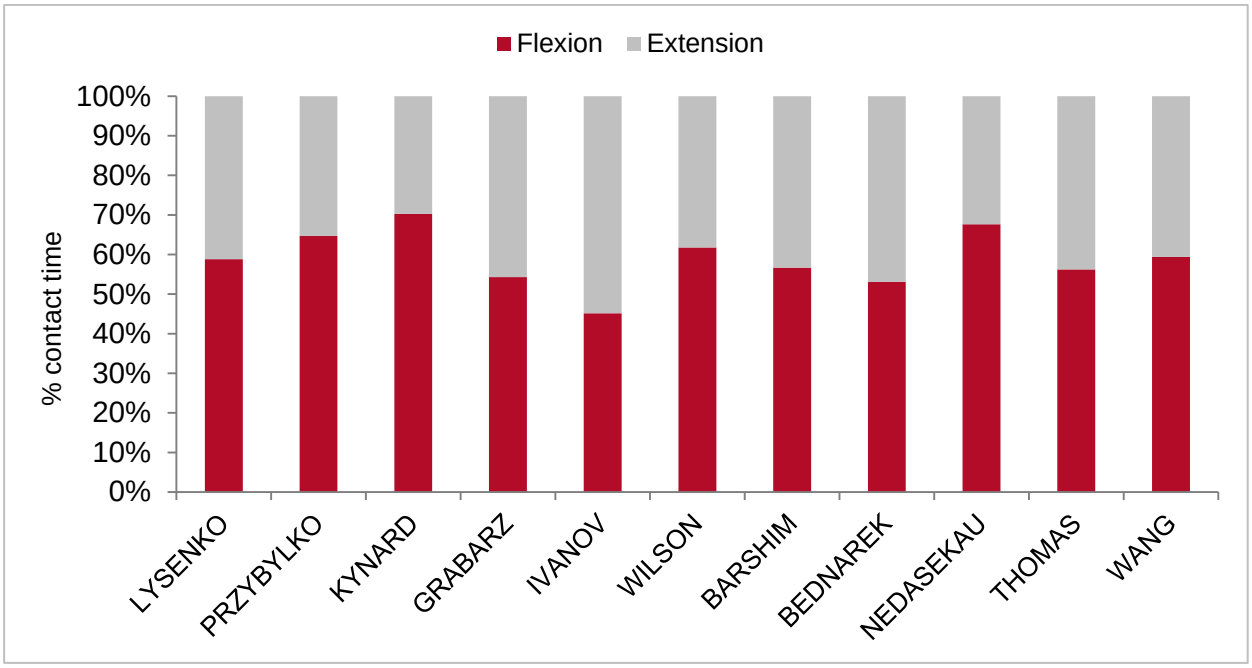

Figure 23. The percentage of time spent during knee flexion and extension during the final foot contact (take-off phase).

The following graphs provide information on the movement synchrony between the hip, knee and ankle joints based on peak angular velocity data.

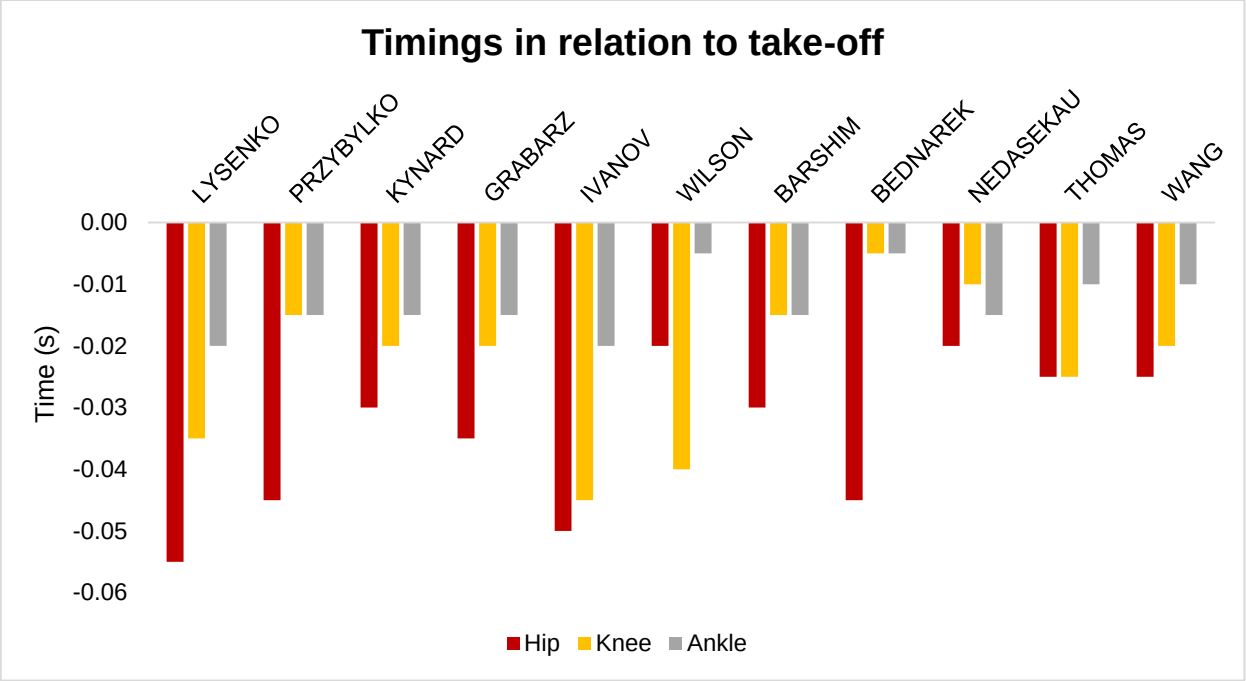

Figure 24. Time difference between peak angular velocity of the hip, knee and ankle and the instant of take-off. Note: minus values indicate time prior to take-off that the respective peaks occurred.

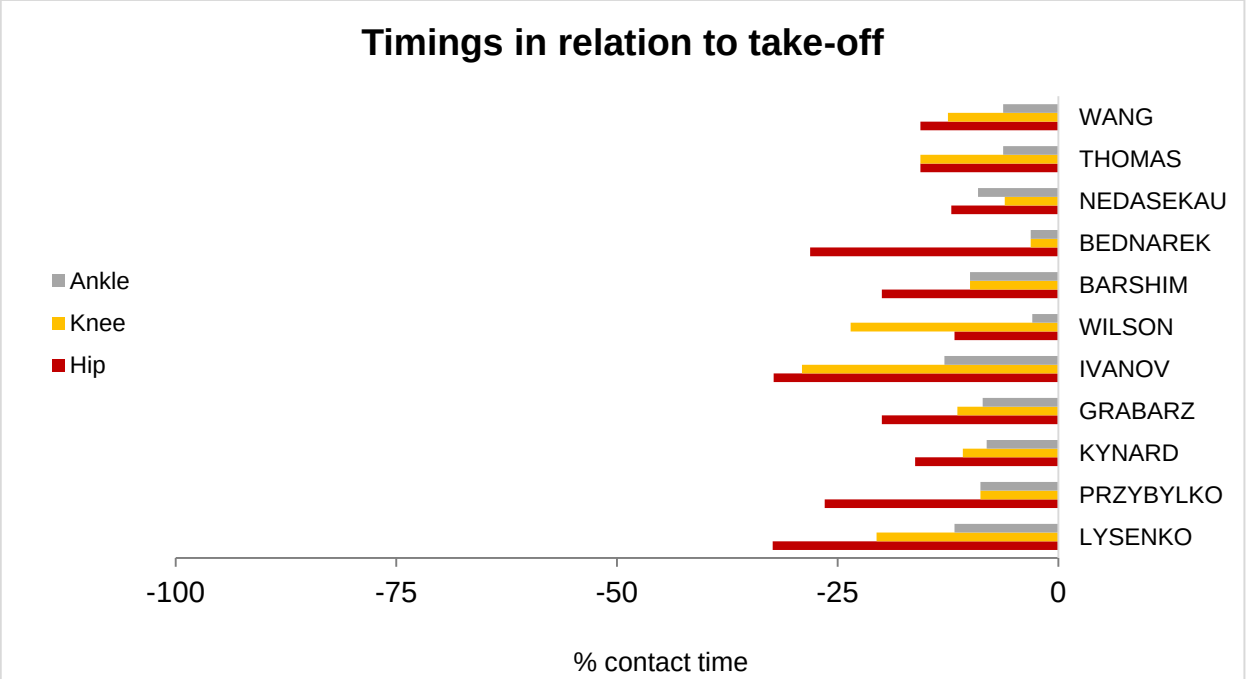

Figure 25. Time difference between peak angular velocity of the hip, knee and ankle and the instant of take-off (expressed as a percentage of take-off contact time). Note: -100% indicates touchdown whilst 0 indicates take-off.

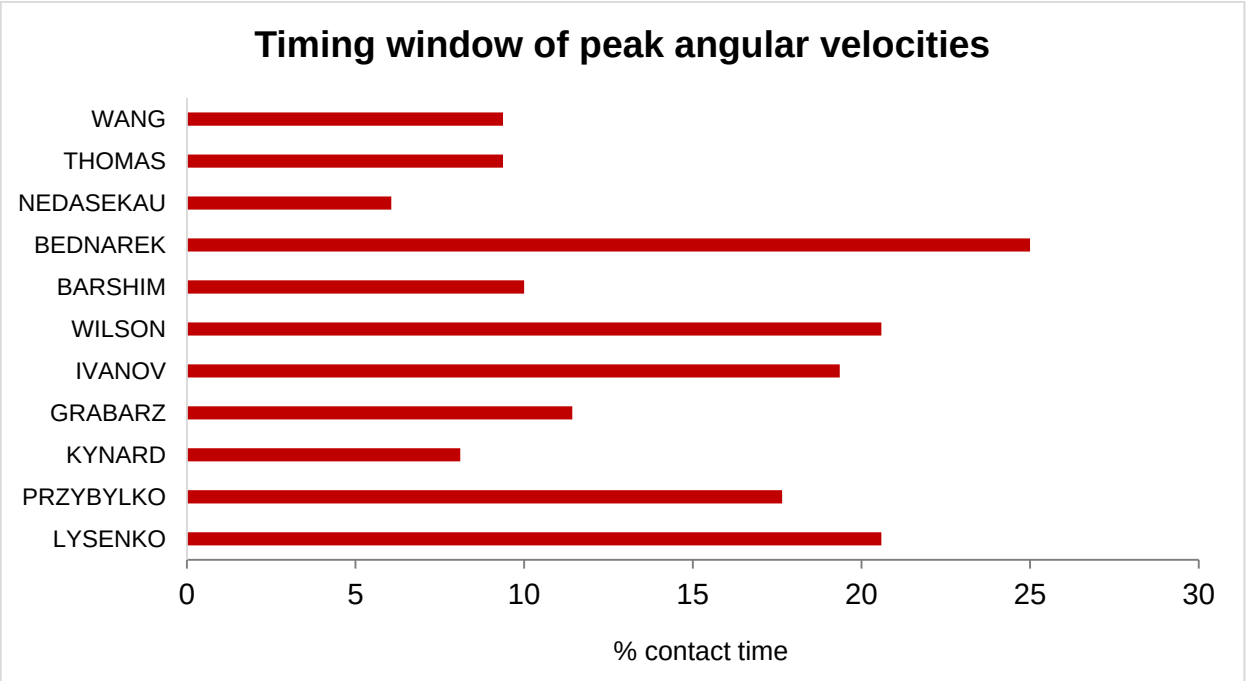

Figure 26. The time difference between the peak hip angular velocity and the peak ankle angular velocity during the take-off phase expressed as a percentage of take-off contact time.

Table 13 below shows the angles of the free hip and knee at touchdown and take-off and also the peak flexion angle of the free knee. Obviously the hip angle is expected to move from an extended to flexed position and the values corroborate this. For the knee, the peak flexion angle provides an indication of athletes which adopt a tightly folded knee position and those that adopt a more extended free limb.

Table 13. The hip and knee (free leg) angles at the instant of touchdown (TD) and toe-off (TO) during the take-off phase as well as the maximum (lowest) knee flexion.

Athlete	Hip angle (°)		Knee angle (°)		
	TD	TO	TD	Lowest	TO
LYSENKO	158	87	98	19	66
BARSHIM	177	99	76	21	58
PRZYBYLKO	167	89	108	32	58
KYNARD	170	95	89	32	98
BEDNAREK	177	97	116	39	72
NEDASEKAU	155	109	121	53	92
THOMAS	162	96	94	25	102
WANG	167	99	92	24	77
GRABARZ	164	103	108	47	95
IVANOV	171	89	92	29	70
WILSON	173	97	93	66	81

Table 14 below shows the whole body and trunk lean at touchdown during the take-off phase as well as the level of shank (shin) lean.

Table 14. The whole-body and trunk lean at touchdown during the take-off phase for each of the athletes. Note: zero degrees indicates a CM over the plant foot/a vertical trunk position/a vertical shank position.

Athlete	Whole body lean at TD (°)	Trunk lean at TD (°)	Shank angle at TD (°)
LYSENKO	38	15	37
BARSHIM	38	14	37
PRZYBYLKO	40	15	46
KYNARD	41	14	41
BEDNAREK	38	21	37
NEDASEKAU	39	21	41
THOMAS	41	15	37
WANG	38	18	41
GRABARZ	41	17	43
IVANOV	34	14	33
WILSON	40	14	38

This page shows the shoulder-hip separation angles at TD and TO during the take-off phase. These values provide an indication of the shoulders position relative to the hips position and consequently the rotation of the trunk around the long axis.

Table 15. Shoulder-hip separation angles at TD and TO during the take-off phase along with the range of motion (ROM) between the two times points.

Athlete	Shoulder-hip separation (°)		
	TD	TO	ROM
LYSENKO	−53	6	59
BARSHIM	−61	11	72
PRZYBYLKO	−59	14	73
KYNARD	−34	15	49
BEDNAREK	−35	37	72
NEDASEKAU	−55	24	79
THOMAS	−50	24	74
WANG	−39	18	57
GRABARZ	−38	10	48
IVANOV	−42	8	50
WILSON	−28	14	42

Note: *A separation angle of 0° indicates parallel alignment of the shoulders and hips whilst an angle of 90° a perpendicular alignment.*

Figure 27 below shows the hip-shoulder positions at TD and TO for each of the athletes. Yellow arrows indicate foot orientation, red markers indicate left and right hip position and blue markers indicate left and right shoulder position.

Lysenko - TD

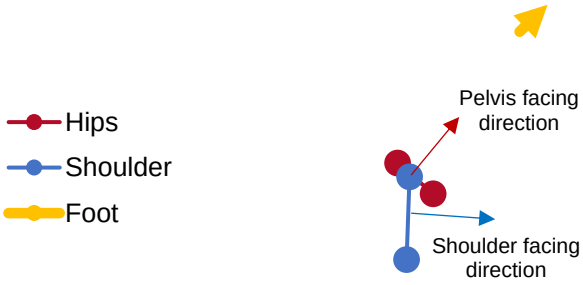

Lysenko - TO

Grabarz - TD

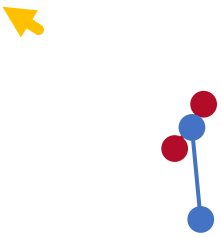

Grabarz - TO

Przybylko - TD

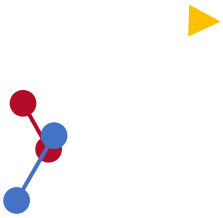

Przybylko - TO

Ivanov - TD

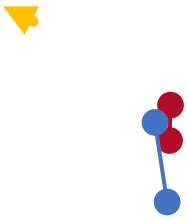

Ivanov - TO

Kynard - TD

Kynard - TO

Barshim - TD

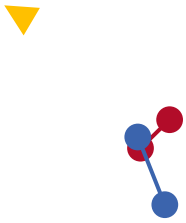

Barshim - TO

Bednarek - TD

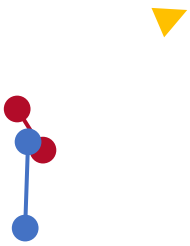

Bednarek - TO

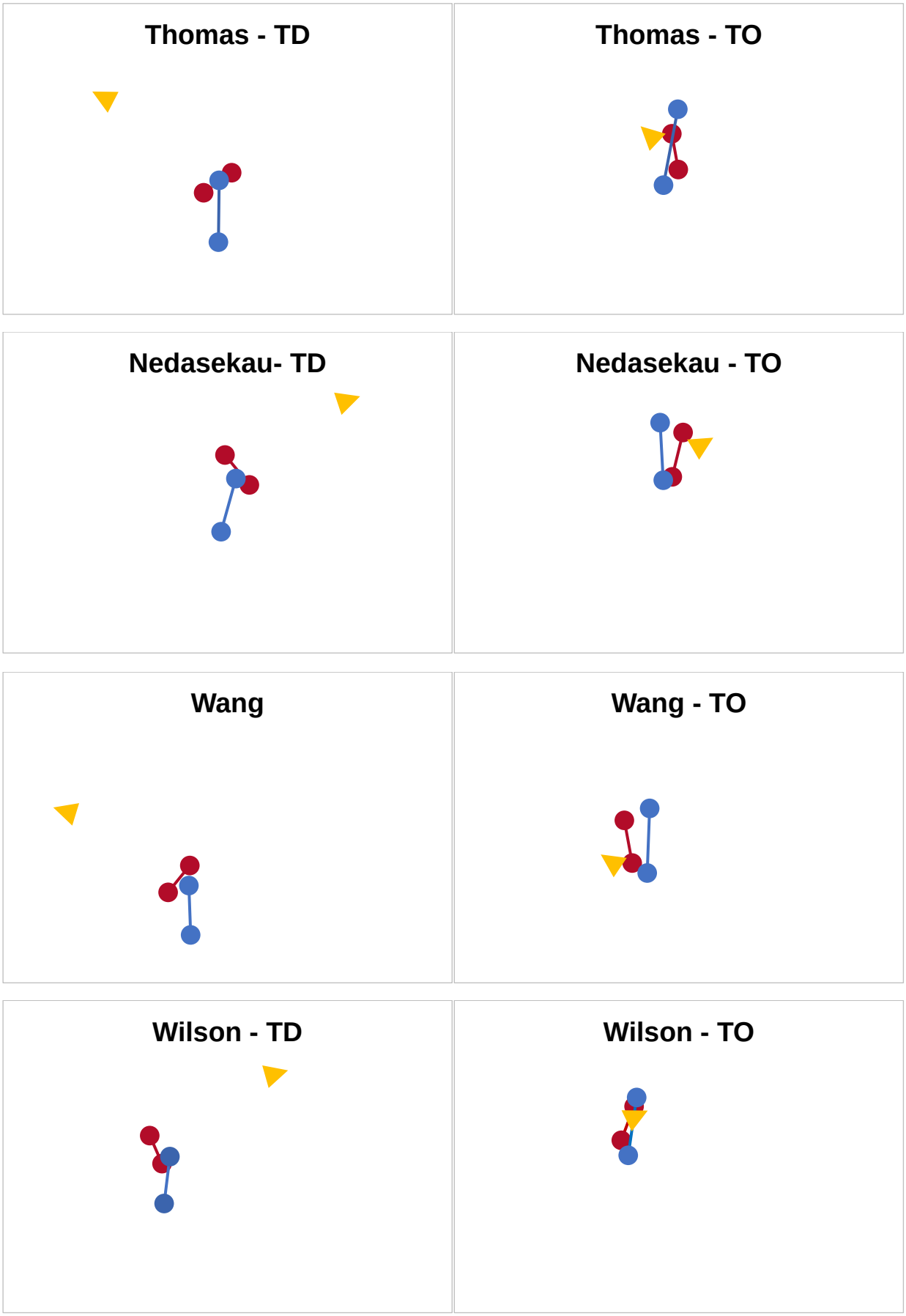

Figure 27. Shoulder (blue lines) and hip (red lines) position relative to the foot (gold) at TD and TO for each of the athletes.

Figure 28 below shows the shoulder-hip separation angle throughout the take-off phase.

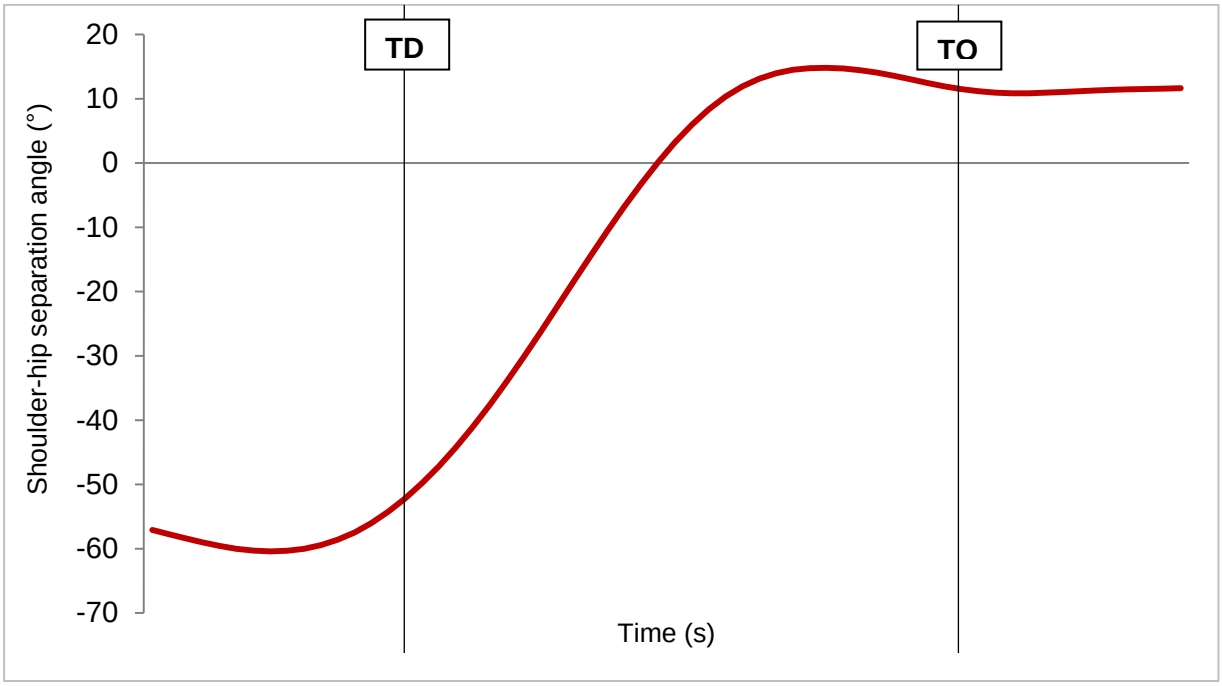

Figure 28. Example of body orientation at TD and TO during the take-off phase for Lysenko.

COACH'S COMMENTARY

Athletes train to produce peak performance in championship competition. Despite the consistent environment afforded by an indoor competition and the fact that the competition was a straight final, by world-class standards the Birmingham Indoor World Championships was a poor competition. Apart from Lysenko and Przybylko athletes all performed well below their best. One possible factor may have been the unforeseen but significant time delay to the published start time to the competition because of ceremonial activity. This highlights that coaches and athletes should prepare for every eventuality.

The aim in the high jump event is for the athlete is to project the entire body over an increasingly raised horizontal fibreglass lath set on two narrow pegs without dislodging it. To be successful the athlete faces several challenges:

- Create sufficient horizontal momentum to pass from one side of the bar to the other.
- Maximise the conversion of horizontal to vertical momentum to raise the body high enough to clear the bar.
- Adjust the body position during the flight so as not to dislodge the bar.

The final part of high jump approach comprising a series of chords is commonly referred to as a "curve". Adopting this approach run pattern is designed to enable the athlete to arrive at the point of take-off with lateral and rearward displacement of the centre of mass (CM) with respect to the final foot contact and with a lowered CM while minimising leg and hip flexion and speed loss. Such a position is intended to allow the athlete to generate the necessary tri-axial angular momentum during the actual takeoff.

Biomechanically the high jump is a complex event. Uniquely when compared to the other three jump events in athletics, an effective take off can be produced over a wide time frame ranging from 0.11 seconds (Dmitrik in Daegu 2011) to 0.20 seconds (Moya in Helsinki 2005). It was interesting to note that in Birmingham the time frame range between the finalists was quite small (0.15 seconds to 0.17 seconds). Additionally the athlete has the freedom to approach the take off point at an angle and speed of their choosing, select a take-off point relative to the bar in order to best generate the forces, vectors and rotations necessary for successful performance.

As in previous biomechanical reports on the high jump there was some noted commonality. All athletes used a "curve" in the last three strides of the approach, displayed rearwards and sideways lean away from the bar, had their shortest flight time between the penultimate and plant contacts (0.04 to 0.07 seconds) and employed a heel first plant contact. All jumpers spent more time in eccentric contraction that in concentric contraction during the takeoff phase.

The recorded data however continued to highlight diversity in technical application between athletes perhaps reflecting the complexity of the event:

- Final Approach run velocities ranged from 8.22 m/s (Przybylko) to 7.33 m/s (Wilson).
- There was again a large range final approach run angles (step-to-bar) from 46.2° (Lysenko) to 21.9° (Przybylko).
- Take-off distance from the bar ranged from 0.90 m (Nedasekau) to 1.54 m (Barshim).
- Approach run angle change (step to bar) during the last stride ranged from five° (Lysenko) to greater than 32° (Kynard and Bednarek) with most athletes in the range of 25-30°. Without full approach data one cannot be certain whether athletes stepped out onto their penultimate contact or tightened their curve into their plant contact.
- One stride before plant, seven athletes touched down ball of foot first, one athlete used a full foot contact and the remaining three used a heel contact (determined visually from video footage).
- In the last three steps of the approach a number of patterns were observed. One athlete used a short/shorter/shortest stride pattern, six of the athletes a short/long/short pattern and three a short/long/longer stride pattern. Data was incomplete for Nedasekau (Table 9).
- The length of the last stride varied from 1.83 m (Wang [who employed a long-short pattern]) to 2.16 m (Przybylko [who used a short-long pattern]).
- Apart from Lysenko and Thomas all athletes recorded increased ground contact times in the final contact of the approach.
- Plant foot instability was still an issue with four of the jumpers displaying over-pronation (determined visually from video footage).
- At take-off contact all athletes loaded varying amounts of negative vertical velocity onto their jump leg. Five athletes recorded amounts in excess of 0.7 m/s while Ivanov possessed hardly any (0.06 m/s). Apart from Ivanov, this loading forced all athletes into further lowering of their centre of mass in the early part of the take-off.
- With the exception of Ivanov all jumpers spent more time in eccentric contraction than in concentric contraction during the take-off phase. Coaches may wish to consider how different levels of eccentric loading can be utilised to provide a positive stimulus in the generation of vertical velocity.
- A variety of different arm actions were noted. One “original Fosbury” running arm action (Thomas), with the other eight finalists all using a double arm shift with both arms being brought forward during the penultimate stride (apart from Przybylko and Ivanov who held back their bar side arm during the penultimate stride). In Birmingham no athlete employed a single barside lead arm.

- Seven athletes employed a tightly folded free knee. Only three athletes (Nedasekau, Grabarz and Wilson) employed an “open knee” free leg swing.
- At peak CM height, locations ranged from 22 centimetres beyond (Lysenko) to 13 centimetres in front of the bar (Wilson) with most jumper’s CM high point falling within 10 centimetres of the bar.

The overhead views illustrating hip and shoulder displacement during the takeoff are interesting (Table 15 and Figure 27). In addition to highlighting the noticeable displacement and ranges of motion between hip and shoulder complexes during the take-off (particularly at final touchdown), it is possible to see how effective, or otherwise, athletes were in taking off above their plant foot. Deliberately adopting such a “torqued” position prior to the high ground reaction forces that act on the body during the takeoff requires careful consideration by coaches. It reinforces the need for precise postural positioning and high levels of conditioning and stability in the musculature of the trunk and spine. There are potential benefits from adopting this position. One is to stimulate a stretch reflex across the hip of the free leg. Correctly timed this can enhance the contribution of the free leg to the take-off. The other is to drive the shoulders and arms up and away from the bar. With the noted differences in range of motion and start and finish alignment in relation to the bar, coaches may wish to consider the relative contribution of the arms and free hip/leg in generating both lift and long axis rotation. As an example Figure 28 highlights Lysenko’s rate and degree of ‘unwinding’ of the hip/shoulder complexes in relation to final touchdown and take-off.

An efficient layout position is one where the trunk crosses the bar at a right angle with the hips elevated in relation to the shoulders and knees. Ideally the shoulder girdle, hip complex and knees should all remain horizontal as they cross the bar. The centre of mass should peak above the bar and the body should possess sufficient angular momentum in flight so that the body rotates around the bar enabling the shoulders to fall towards the mat and the knees and feet to lift to clear the bar. As can be seen in Table 4 and Figure 7, such an ideal position is rarely achieved. Many issues of alignment and rotation can be tracked back to less than perfect positioning and angular momentum generation during the take-off.

It is interesting to compare Lysenko’s London and Birmingham performances. In London and Birmingham he approached the bar in a similar pattern with a gently curving approach typified by gradually decreasing stride length and increasing stride rhythm making only small step-to-step angle changes. Although he took off a little further away and narrowed his final step-to-bar angle by some 5° in Birmingham, the peak position of his CM was still positioned well beyond the line of the bar by 22 centimetres. In comparison to London his final approach speed was reasonably faster. There was a measurable increase in rhythm and decreased flight time during his last three steps of the run. At plant he possessed some 6° less rearwards trunk lean and entered the takeoff

with a fractionally higher CM. This probably resulted in his less steep flight trajectory than in London.

Compared to London a number of differences were noted at take-off. Despite his faster speed and rhythm of his final approach steps, increased negative vertical velocity at final touchdown and a slightly longer eccentric phase in the take-off, he was able to reduce the amount of knee flexion by 17°, ankle flexion by 4° and also generated 4° of increased knee extension at take-off. Throughout the takeoff his plant foot remained stable. Lysenko was able to complete his take-off within the same time frame as London (0.17 seconds), generating greater vertical velocity (4.97 m/s versus 4.76 m/s).

In comparison to all the other finalists, his reduced CM attack angle resulted in his CM being laterally displaced with respect to this plant foot at take-off (Figure 14). This in combination with his increased level of plant leg stiffness and long free limb acceleration allowed him to raise his CM to an impressive 2.47 m, 7 cm higher than in London and some 11 cm above the height of his winning clearance. His bar clearance position however is still capable of great improvement as he adopted a very flat layout with no real hip extension (Table 4) at peak CM height. With noticeable greater travel after take-off (Figure 6), at critical heights in particular, this jumper may benefit from adjustment to his take-off location and take-off angle in order to consistently position his CM directly above the bar and lessen the risk of hitting and dislodging the bar from the pegs.

Barshim's gently curving approach allows him to run quickly. Although faster at touchdown than in London (7.66 m/s versus 7.46 m/s), his loss in horizontal velocity from touchdown to take-off was greater a factor possibly resulting in his CM peaking 6 centimetres before the bar (London was 0 cm). He also displayed a slightly higher final (step-to-bar) angle (>40°) with a long/short pattern in the last two strides that required a distant take-off (> 1.54 m) from the bar. His take-off contact was short at 0.15 seconds but 0.01 sec longer than in London. The data in Table 15 shows how he was able to generate significant long-axis rotation to orientate and place his high point above the bar. At the end of the approach on his silver medal winning jump Barshim made a final step-to-bar angle change of some 25° (Table 7) which is greater than normal for him. His final CM attack angle was also slightly higher than in London, allowing his CM to pass behind and to the barside of his plant foot.

Above the bar he was able to demonstrate an efficient "layout position" with his CM (2.37 m) only 4 centimetres above the bar to maximise his centre of mass height. Compared to London his take-off leg flexed a little more but concentrically his knee was able to work over a larger range of motion. In comparison to Lysenko and Przybylko, his hips, knees and ankle reached peak angular velocity (concentric) within a smaller time window and closer to take-off (Figures 24-26). These factors indicated excellent levels of joint synchronisation and timing which may be factors

contributing to his ability to generate high vertical take-off velocities. Of all the jumpers he displayed the highest ratio of flight time to contact time (Figure 22) which like London, may be indicative of his high levels of lower-body stiffness.

The bronze medalist Przybylko, the fastest on the approach in London, was again easily the fastest jumper of the finalists (8.22 m/s). He also had the narrowest final step-to-bar angle of all the finalists <22°, some 4° more parallel to the bar than in London and he took off some 16 centimetres closer to the bar. With his CM attack angle only 6° greater than his final step-to-bar angle, his CM reached its high point some 8 centimetres in front of the bar whereas in London his peak CM was some 5 centimetres behind the bar.

At touchdown he possessed greater whole-body lean but slightly less rearwards trunk lean in comparison to London. He also displayed increased stiffness in his take-off leg with 5° less knee flexion and 6° less ankle flexion and was able to develop an additional 6° of knee extension at the end of the take-off contact. Entering the take-off with slightly increased negative vertical velocity, his take-off took slightly longer than London (0.01 seconds) but he was able to generate greater vertical velocity (4.72 m/s versus to 4.68 m/s) raising his CM to a similar height to London (2.32 m versus 2.31 m).

One of the effects of this wide angle of approach was that his timing above the bar was critical. His great speed, the wide angle of approach, a large degree of lean, a highly ‘torqued’ position and long last step resulted in his plant foot being everted from the bar demonstrating a large degree of pronation during the takeoff. These factors may have contributed to his longer eccentric phase during the take-off. Above the bar his hip extension was efficient with his CM passing only 3 centimetres above he bar, However one consequence of his extreme take-off position and alignment meant he spent more time above the bar and crossed it at an angle giving him a reduced margin for error.

As might be expected we see the more successful jumpers better able to utilise their final horizontal approach velocity (Table 10). Barshim and Lysenko in particular were noticeably more effective in converting their horizontal speed into vertical velocity (velocity transfer).While the ability to development vertical velocity is critical to the successful performance of the event, the fact that all three medalists utilised greatly differing techniques yet again confirms the fact that it is possible to posses differing physiques and use a variety of technical interpretations and still be successful. This still leaves the challenge for the coach is to carefully determine and develop the technique and physicality that bests suits the makeup of their athlete.

CONTRIBUTORS

Dr Gareth Nicholson is a Senior Lecturer in Sport and Exercise Biomechanics at Leeds Beckett University and is Course Leader for the MSc Sport & Exercise Biomechanics pathway. Gareth has First Class Honours in BSc Sport and Exercise Science as well as an MSc in Sport & Exercise Science and a PhD from Leeds Beckett University. Gareth's research interests are in the measurement and development of strength and power. Gareth currently supervises a range of health and performance-related research projects.

Dr Tim Bennett is a Senior Lecturer in Sport and Exercise Biomechanics. His research interests are in the area of striking sports, particularly soccer kicking analysis. He is also interested in motor control and human movement variability and this can influence sports performance under varying task constraints. Tim is also involved in golf and throwing research projects, which aim to provide a better understanding of human movement and performance.

Dr Athanassios Bissas is the Head of the Biomechanics Department in the Carnegie School of Sport at Leeds Beckett University. His research includes a range of topics but his main expertise is in the areas of biomechanics of sprint running, neuromuscular adaptations to resistance training, and measurement and evaluation of strength and power. Dr Bissas has supervised a vast range of research projects whilst having a number of successful completions at PhD level. Together with his team he has produced over 100 research outputs and he is actively involved in research projects with institutions across Europe.

A retired Head of Physical Education, Denis Doyle is an IAAF Level Five Elite Jumps coach and holds numerous UKA Level Four Performance Coach Awards. He currently works in Coach Development Roles with England and Welsh Athletics. He has coached for 50 years across all sectors of the sport and has experience as a team manager for Great Britain and England and as a coach with British, Irish and Indian teams at four Olympics and six World Championships. His personal coaching record includes guiding over thirty five athletes from several nations to international success, five at Olympic level, with ten of them setting national senior and age group records. He is coach to 2017 European Junior High Jump Bronze Medalist Tom Gale.